THE ASTROPHYSICAL JOURNAL, 291:356–376, 1985 April 1

NONLINEAR SPIRAL DENSITY WAVES: AN INVISCID THEORY

FRANK H. SHU
Astronomy Department, University of California, Berkeley
AND
CHI YUAN[1,2] AND JACK J. LISSAUER[1]
NASA/Ames Research Center
Received 1984 August 6; accepted 1984 October 17

ABSTRACT

We develop an inviscid fluid theory for nonlinear self-gravitating spiral density waves that adopts, for simplicity, the most stringent of the asymptotic approximations normally used, but relaxes the assumption of small amplitude. Our treatment allows the consideration of both free wave trains and those excited by resonant forcing. In a frame which corotates with the pattern, the pressure-free problem reduces in a Lagrangian description to the solution of a complex nonlinear integral equation. A nonlinear dispersion relation and an angular momentum conservation relation can be derived for the far wave zone where WKBJ approximation methods apply. Guided by this result and by earlier work on the linear theory of density waves, we are able to write down a heuristic ordinary differential equation that mimics many of the properties of the integral equation. Numerical solutions of the former are easily obtained for forced density waves of the strengths typically seen in Saturn's rings. These numerical solutions, when substituted back into the integral equation, satisfy the latter to acceptable accuracy for practical work, even in the near wave zone where most of the resonant coupling takes place.

Although meaningful detailed comparisons with observations of the density waves in Saturn's rings will require the inclusion of wave damping by induced viscous stresses, the theory developed herein already has several important implications. First, the nonlinear torques exerted by the satellites orbiting Saturn are not very different from those calculated by the linear theory; therefore, the existing difficulty with short lifetimes in the Saturn system does not have an escape in this direction. Second, even without the inclusion of pressure or viscous stresses, neighboring streamlines never cross, although they come arbitrarily close in the asymptotic wave regime. The theoretical wave profiles are qualitatively similar to the broad, shallow troughs and sharp symmetric peaks that are seen in many of the *Voyager* frames of nonlinear density waves in Saturn's rings. Third, the incorporation of the effects of pressure is easy, opening the way for the development of a theory of nonlinear density waves that would be applicable to spiral galaxies.

Subject headings: hydrodynamics — planets: Saturn

I. INTRODUCTION

The theory of spiral density waves, invented to explain the spiral structure of disk galaxies (Lindblad 1963; Lin and Shu 1964; Toomre 1977; Bertin 1980), has also been found useful for the study of planetary rings (Goldreich and Tremaine 1978; Cuzzi, Lissauer, and Shu 1981). The linear theory is by now well developed, in regard to both self-excited modes (see, e.g., Toomre 1981; Lin and Bertin 1984) and resonantly forced waves (see, e.g., Goldreich and Tremaine 1979; Shu 1984). The nonlinear theory is less complete; fully nonlinear calculations (e.g., Roberts 1969; Sanders and Huntley 1976) usually consider only locally forced waves in a gaseous medium which is itself not self-gravitating (an exception is the study of S. Balbus, L. Cowie, and S. Lubow 1983, private communication). Some large-scale numerical simulations do consider self-gravitating disturbances (e.g., Miller, Prendergast, and Quirk 1970; Hohl 1971; Woodward 1980; Sellwood and Carlberg 1984), but the transitory nature of the results makes them difficult to interpret, especially with respect to the effects that are unique to the nonlinear problem. Analytical calculations which include self-gravitation have, so far, obtained results only in the slightly nonlinear regime (e.g., Vandervoort 1971), or have concentrated on partial effects (e.g., the modification of the epicyclic frequency, Norman 1978) that are not of primary importance to the physical problem at hand. In the present paper, we remedy these shortcomings.

In this first study, we shall adopt the simplest asymptotic ordering which can still yield useful results. When we come to include the effects of random motions, we shall use an isothermal fluid model for the matter in the disk (for a discussion of the merits and drawbacks of a fluid description for stellar disks see Lin and Lau 1979). In the fluid model, let $c(r)$ be the isothermal sound speed at a radius r in a disk where the unperturbed surface density and epicyclic frequency are $\sigma_0(r)$ and $\kappa(r)$. If the axisymmetric gravitational field of the disk is a small fraction of the overall field, and if the epicyclic excursion of a typical free particle is a small fraction of the radius r, the nondimensional quantities

$$\delta_1 \equiv \frac{\pi G\sigma_0(r)}{r\kappa^2(r)} \quad \text{and} \quad \delta_2 \equiv \frac{c(r)}{r\kappa(r)} \tag{1}$$

will be very small compared with unity. In Saturn's rings they are of order 10^{-8}, but in disk galaxies they can be of order

[1] NAS–NRC Resident Research Associate.
[2] On leave from Physics Department, City College, City University of New York.

10^{-1} or larger. The ratio of these two quantities,

$$Q \equiv \frac{\delta_2}{\delta_1} = \frac{\kappa c}{\pi G \sigma_0} , \tag{2}$$

is the fluid analog of Toomre's (1964) stability parameter and must exceed unity in a galactic disk if it is to be stable to axisymmetric disturbances of all scales. (In planetary rings, the finite size of the particles can provide a stabilizing influence even if $Q = 0$; see Shu 1984.)

When δ_1 and δ_2 are $\ll 1$, it becomes possible to consider tightly wound self-gravitating spiral disturbances in the disk where the azimuthal variation is much less rapid than the radial one. To be more precise, if the pattern is m times periodic in θ, so that m/r is the azimuthal wavenumber, and if $|k| = 2\pi/\lambda$ is the radial wavenumber, where λ is the radial spacing between successive crests, then we may adopt the WKBJ approximation,

$$\frac{m}{|k| r} \ll 1 , \tag{3}$$

for tightly wound spiral waves. The utility of the approximation (3) is controversial in galactic dynamics (which has motivated techniques to relax it, at least within the context of the linear theory), but it holds to a very high order of approximation in Saturn's rings.

Within the context of the above discussion, there are two distinct regimes in which a forced disturbance can be considered to be nonlinear. In the first regime, the external forcing is strong enough to cause radial excursions of fluid elements that are comparable to r itself. This can happen for interacting galaxies (see, e.g., the simulations of Toomre and Toomre 1972), but never applies to planetary rings, since the satellites of the giant planets are all much less massive than the central body. In the second regime, the external forcing is strong enough to cause radial excursions of fluid elements that are comparable to the inverse wavenumber $|k|^{-1} \equiv \lambda/2\pi$ of the density waves which are excited. The crests of the density waves can steepen considerably if a large fraction of the matter on either side of a crest crashes in the middle; galactic shocks are the most familiar manifestation of this phenomenon (see, e.g., Shu, Milione, and Roberts 1973). This type of nonlinearity (see Fig. 1) is also encountered in Saturn's rings; although the closer moons are tiny compared with the planet, they have masses that are not negligible in comparison with the mass of the ring system (cf. eq. [36]). To have enough angular momentum luminosity to carry away the secular torques exerted by the moons at the Lindblad resonances, the density waves excited in Saturn's rings often have to be very nonlinear.

Our discussion of nonlinear effects is restricted to the second of the types listed above. As we shall see in the next section, this restriction allows us to make considerable analytic progress.

Before we begin our formal deliberations, however, we should remark that the basic results derived in this paper could have been obtained by very different methods using the discrete streamline approach of Borderies, Goldreich, and Tremaine (1983*a*) and taking the appropriate continuum limit. Indeed, Goldreich and Tremaine (1983, private communication) have shown that the fundamental nonlinear integral equation (48) of this paper would follow also from their formalism if they had made full use of the asymptotic approximation invoked here. This convergence of results adds confidence to our basic approach.

II. MATHEMATICAL FORMULATION

a) Basic Equations

We begin our analysis by ignoring, at first, the presence of pressure and viscous stresses. A Lagrangian description is then natural, since the characteristic equations associated with the Eulerian description are just the orbit equations of a free particle. If the motions are restricted to a plane, the dynamical equations read:

$$\frac{d^2 r}{dt^2} = \frac{J^2}{r^3} - \frac{\partial V}{\partial r} , \tag{4a}$$

$$\frac{dJ}{dt} = -\frac{\partial V}{\partial \theta} , \tag{4b}$$

$$\frac{d\theta}{dt} = \frac{J}{r^2} , \tag{4c}$$

where the total gravitational potential V is a sum of contributions from the planet, the moon, and the disk (for a galaxy these would be the bulge-halo, a satellite galaxy, and the disk):

$$V(r, \theta, t) = V_P(r) + V_M(r, \theta, t) + V_D(r, \theta, t) . \tag{5}$$

For V_M we are interested only in a particular Fourier component of the moon's gravitational potential:

$$V_M(r, \theta, t) = \phi_M(r) \cos(\omega t - m\theta) . \tag{6}$$

For $m \neq 0$, V_M is time-independent in a frame of reference

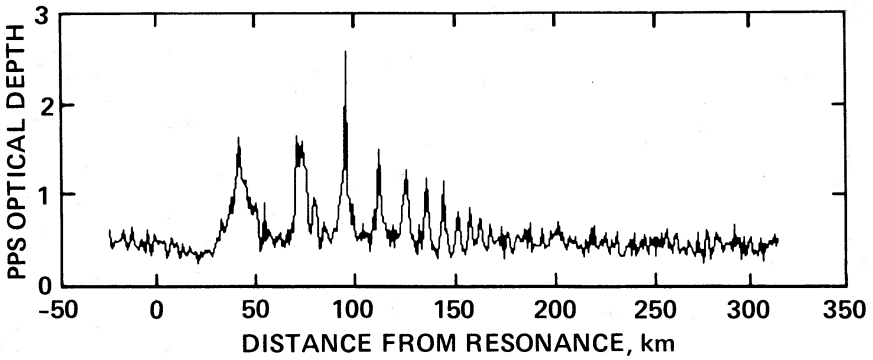

FIG. 1.—Nonlinear spiral density wave excited in Saturn's rings near a location where the ring particles orbit Saturn five times for each three times that the satellite Mimas does. In the planetary rings literature, this is referred to as the 5:3 density wave associated with Mimas. (Optical depth scan courtesy of L. W. Esposito).

which rotates with angular velocity $\Omega_p \equiv \omega/m$, i.e., in a frame where we measure the azimuthal angle according to

$$\varphi \equiv \theta - \Omega_p t \, . \tag{7}$$

In a steady state, the forcing potential (6) will result in disturbances which are functions only of r and φ. The induced changes in specific energy, E, and specific angular momentum, J, are related to one another, since Jacobi's integral

$$H \equiv E - \Omega_p J \tag{8}$$

is a strict constant of the motion. Thus, $\dot{E} = \Omega_p \dot{J}$, and it suffices for us to follow angular momentum changes only (see, e.g., Lynden-Bell and Kalnajs 1972).

Given our discussion in § I, we are motivated to look for solutions in the perturbation form,

$$r = r_0 + r_1 \, , \tag{9}$$

where the unperturbed position r_0 is related to the unperturbed specific angular momentum J_0 by

$$r_0^2 \Omega(r_0) = J_0 \, , \tag{10}$$

where Ω is the angular frequency required for centrifugal balance against the planet alone:

$$r_0 \Omega^2(r_0) \equiv \frac{dV_P}{dr}(r_0) \, . \tag{11}$$

As we discuss later (see footnote 3), it is possible to renormalize the right-hand side of equation (11) to include the axisymmetric contributions of the disk and all of the satellites. (This is more important in the galactic context than in the planetary one.) Without this renormalization, we are considering the planet without moons and self-gravitating rings to be the reference state.

If we separate the specific angular momentum by writing

$$J = J_0 + J_1 \, , \tag{12}$$

then assume $r_1 \ll r_0$ and $J_1 \ll J_0$, we may expand all functions which are smoothly varying in r about r_0. Since $|k| r_1$ is *not* small in comparison with unity in a nonlinear density wave of radial wavenumber k, we do *not* expand $V_D(r_0 + r_1, \varphi)$ about r_0. On the other hand, the azimuthal variation of V_D is slow in comparison with its radial variation, so it helps to write φ as

$$\varphi = \varphi_0 + [\Omega(r_0) - \Omega_p]t + \varphi_1 \, , \tag{13}$$

where φ_0 is a constant and φ_1 may be considered to be a small perturbation about the mean circular motion. The perturbational equations for the orbit trajectories now read:

$$\frac{d^2 r_1}{dt^2} + \kappa^2(r_0) r_1 = 2\Omega(r_0) \frac{J_1}{r_0} - \frac{\partial V_M}{\partial r} - \frac{\partial V_D}{\partial r} \, , \tag{14a}$$

$$r_0^2 \frac{d\varphi_1}{dt} = J_1 - 2 r_0 \Omega(r_0) r_1 \, , \tag{14b}$$

$$\frac{dJ_1}{dt} = -\frac{\partial V_M}{\partial \varphi} - \frac{\partial V_D}{\partial \varphi} \, , \tag{14c}$$

where

$$\kappa^2(r_0) \equiv \frac{1}{r_0^3} \frac{d}{dr_0} [r_0^4 \Omega^2(r_0)] \tag{15}$$

is the square of the epicyclic frequency and does not equal $\Omega^2(r_0)$ for an oblate planet (or a disk galaxy). In equations (14a)–(14c), the slow (rapid) variation of V_M (V_D) with changes in r imply that the derivatives of V_M can be evaluated at $(r_0, \varphi_0 + [\Omega(r_0) - \Omega_p]t)$, but those of V_D must be evaluated at $(r_0 + r_1, \varphi_0 + [\Omega(r_0) - \Omega_p]t)$.

Our ability to expand V_D in φ, but not in r, assumes tightly wrapped waves where the φ-derivatives of V_D are negligible in comparison with its r-derivatives. Consistent with this *asymptotic* approximation, equation (14c) may be integrated (except near corotation, where $\Omega = \Omega_p$) to yield

$$J_1 = \frac{\phi_M(r_0)}{\Omega_p - \Omega(r_0)} \cos \psi_0 \, , \tag{16}$$

where ψ_0 is the phase of the moon's potential encountered on the unperturbed circular orbit of a ring particle (cf. eq. [6]):

$$\psi_0 \equiv m\varphi_0 - [\omega - m\Omega(r_0)]t \, . \tag{17}$$

For the steady state response, we look for solutions of r_1 and φ_1 in equations (14a) and (14b) that are periodic in ψ_0. The time derivatives in these equations are taken holding the Lagrangian labels r_0 and φ_0 constant; thus, if we use ψ_0 as a variable to replace t, we may write the equation of motion for r_1 as

$$[\omega - m\Omega(r_0)]^2 \frac{\partial^2 r_1}{\partial \psi_0^2} + \kappa^2(r_0) r_1 = g_D + g_M \, , \tag{18}$$

where g_M is the effective perturbational gravity of the moon's forcing,

$$g_M(r_0, \psi_0) = \frac{1}{r_0} \Psi_M(r_0) \cos \psi_0 \, , \tag{19}$$

with

$$\Psi_M(r_0) \equiv -r_0 \frac{d\phi_M}{dr_0} + \frac{2m\Omega(r_0)\phi_M(r_0)}{\omega - m\Omega(r_0)} \, , \tag{20}$$

and where g_D is the radial self-gravity of the rings. To the asymptotic order of interest in this paper, we may calculate g_D as the gravitational field due to a local collection of straight wires (see, e.g., Borderies, Goldreich, and Tremaine 1983*a*; Shu 1984):

$$g_D(r_0, \psi_0) = -2G \int_0^\infty \frac{\sigma(r', \psi_0)}{r - r'} \, dr' \, , \tag{21}$$

with

$$r = r_0 + r_1(r_0, \psi_0) \, .$$

To obtain the surface density σ, we note that the Lagrangian form of the equation of continuity, with $\psi = m\varphi$, reads:

$$\sigma(r, \psi) r dr d\psi = \sigma_0(r_0) r_0 \, dr_0 \, d\psi_0 \, , \tag{22}$$

expressing the conservation of mass of a fluid element of unperturbed surface mass density $\sigma_0(r_0)$ and area $r_0 \, dr_0 \, d\psi_0$ which has been distorted to surface density $\sigma(r, \psi)$ and area $r dr d\psi$. To the order of asymptotic accuracy which we are consistently working, the ψ-distortions are much less important than the r-distortions, i.e., $d\psi \approx d\psi_0$, and the Jacobian of the transformation becomes

$$\frac{\partial(r, \psi)}{\partial(r_0, \psi_0)} \approx \frac{\partial r}{\partial r_0} = 1 + \frac{\partial r_1}{\partial r_0} \, , \tag{23}$$

when we write r as $r_0 + r_1$. To this order, therefore, we have

$$\sigma(r, \psi) = \frac{\sigma_0(r_0)}{1 + \partial r_1/\partial r_0}, \tag{24}$$

with $\partial r_1/\partial r_0$ being of order unity for a nonlinear wave.

If we change to r_0 and ψ_0 as the independent variables, and if we assume that r_1 varies much more rapidly with r_0 than does $\sigma_0(r_0)$, equation (21) becomes

$$g_D = -2G\sigma_0(r_0) \int_0^\infty \frac{dr_0'}{r_0 + r_1(r_0, \psi_0) - r_0' - r_1(r_0', \psi_0)}. \tag{25}$$

Clearly, most of the contribution to the above integral comes from the neighborhood of $r_0' = r_0$. Indeed, the strong opposing pulls of matter on either side of r_0 requires us to interpret this integral in the principal-value sense if we are to retain the approximation of an infinitesimally thin disk.

With g_D given by equation (25) and g_M by equation (19), equation (18) may be regarded as the equations of motion (in ψ_0) for a set of harmonic oscillators whose displacements r_1 are externally forced by the moon's gravity g_M and which are coupled (in r_0) by the oscillators' self-gravity g_D. Because the advective terms in an Eulerian description are absorbed by using total time derivatives in an Lagrangian formulation and because $r_1 \ll r_0$, nonlinearity enters solely in the term g_D. In principle, after equation (18) has been solved for r_1, as a function of r_0 and ψ_0, the angular displacement φ_1 could be obtained by integrating equation (14b), i.e.,

$$-r_0^2[\omega - m\Omega(r_0)] \frac{\partial \varphi_1}{\partial \psi_0} = \frac{m\phi_M(r_0)}{\omega - m\Omega(r_0)} \cos \psi_0 - 2r_0 \Omega(r_0) r_1 . \tag{26}$$

In practice, this integration is not necessary if the primary quantity of observational interest is the surface density distribution (24).

b) *Reduction to Nonlinear Integral Equation in a Single Variable*

To motivate a simplification of equation (18), we refer to the linear theory, which shows good coupling to the *external* force field only near a Lindblad resonance. In the linear theory, the disturbances are sinusoidal in angular phase, i.e.,

$$\frac{\partial^2 r_1}{\partial \psi_0^2} = -r_1 , \tag{27}$$

and we expect this to hold even in the current problem (an assumption made at the outset in the treatments of resonantly truncated disk edges by Borderies, Goldreich, and Tremaine 1982) because nonlinearities enter only in the second sense of the discussion of § I. To see this formally, add and subtract $[\omega - m\Omega(r_0)]^2 r_1$ on the left-hand side of equation (18):

$$(\omega - m\Omega)^2 \left(\frac{\partial^2 r_1}{\partial \psi_0^2} + r_1 \right) + D r_1 = g_D + \frac{1}{r_0} \Psi_M \cos \psi_0 , \tag{28}$$

where

$$D \equiv \kappa^2(r_0) - [\omega - m\Omega(r_0)]^2 \tag{29}$$

is the usual measure of the distance from Lindblad resonance in frequency space. Let the Lagrangian coordinate

$$x_0 \equiv (r_0 - r_L)/r_L \tag{30}$$

be the fractional radial distance from Lindblad resonance r_L where D is zero. For small x_0, we expand

$$D = \mathscr{D} x_0 , \tag{31}$$

with

$$\mathscr{D} \equiv \left[r_0 \frac{dD}{dr_0} \right]_{r_0 = r_L} . \tag{32}$$

For $m \neq 1$, $\mathscr{D}$ has the value $-3(1 \pm m)\Omega^2(r_L)$ in a Keplerian disk, with the plus sign applying to outer Lindblad resonances and the minus sign to inner ones. Henceforth, we specialize to the case of inner Lindblad resonances where $\mathscr{D} > 0$, the generalization to outer Lindblad resonances being trivial. Thus the parameter

$$\epsilon = \frac{2\pi G \sigma_0(r_L)}{r_L \mathscr{D}} \tag{33}$$

is positive, generally of order δ_1, and very small in planetary rings.

The typical fractional displacements of concern near resonance are of order $\epsilon^{1/2}$; thus, we are further motivated to scale

$$x_0 \equiv \epsilon^{1/2} \xi_0 , \quad r_1 \equiv r_L \epsilon^{1/2} X . \tag{34}$$

In the dimensionless Lagrangian displacement X and fluid particle label ξ_0, we may now write the expanded form of equation (28), for $\epsilon \ll 1$, as[3]

$$\epsilon^{-1/2} \frac{\kappa^2}{\mathscr{D}} \left(\frac{\partial^2 X}{\partial \psi_0^2} + X \right) + \xi_0 X = f \cos \psi_0 - \frac{1}{\pi} \int_{-\infty}^{\infty} \frac{d\xi_0'}{\xi_0 + X - \xi_0' - X'} , \tag{35}$$

where we have defined

$$f \equiv \frac{\Psi_M(r_L)}{2\pi G r_L \sigma_0(r_L)} \tag{36}$$

to be the nondimensional external forcing (taken to be real and positive), and where we have used the shorthand notations X for $X(\xi_0, \psi_0)$ and X' for $X(\xi_0', \psi_0)$.

We expect nonlinear effects to dominate if the parameter f, which is proportional to the ratio of the moon's mass to the disk's mass, is not $\ll 1$. Table 1 gives examples of the values of f applicable to some of the observed density waves in Saturn's rings. Clearly, linear theory would not realistically model many of these waves (see also Esposito, O'Callaghan, and West 1983).

Nevertheless, a simplification is possible in equation (35) because the other nondimensional parameter, ϵ, which is proportional to the ratio of the disk's mass to the planet's mass, *is*

[3] Notice that if $X \equiv 0$ everywhere, then the self-gravity integral on the right-hand side vanishes if we interpret the integral in the principal-value sense. Our asymptotic approximation therefore ignores the long-range effects which would make unequal the pulls of the parts of the *unperturbed* disk which are interior and exterior to the radius corresponding to ξ_0. This effective renormalization means that we may, if we like, include the axisymmetric contributions of the disk (and the satellite systems) in the computations of Ω, κ, etc (cf. discussion in § I). The desirability of taking this approach (rather than starting with $\sigma - \sigma_0$ instead of σ in eq. [21]) was pointed out to us by Scott Tremaine (1983, private communication).

TABLE 1

SOME RESONANCE STRENGTHS IN SATURN'S RINGS

Moon	Resonance Label	Resonance Location r_L (Saturn radii)	Forcing Strength[a] f
Mimas	5:3	2.1929	0.17
	8:5	2.2522	0.02
Janus (larger co-orbital)	2:1	1.5953	0.24
	6:5	2.2255	0.63
Inner F ring Shepherd	10:9	2.1549	0.20
	27:26	2.2533	0.52

[a] These f-values assume a surface density equal to 50 g cm^{-2}. All other parameters are from Lissauer and Cuzzi (1982).

$\ll 1$. This allows us to attempt a solution in the form of a parameter expansion:

$$X = X_1 + \epsilon^{1/2} X_2 + \epsilon X_3 + \cdots , \tag{37}$$

yielding to lowest order for equation (35),

$$\frac{\partial^2 X_1}{\partial \psi_0^2} + X_1 = 0 . \tag{38}$$

The above has the general solution

$$X_1 = A(\xi_0) \cos [\psi_0 - \Phi(\xi_0)] , \tag{39}$$

where the amplitude A and phase Φ are to be determined as real functions of the Lagrangian label ξ_0 (proportional to the unperturbed radial distance from resonance). Equation (39) shows the angular dependence of the Lagrangian displacement X to be strictly sinusoidal to lowest asymptotic order in ϵ (as long as f is of order unity in comparison with $\epsilon^{-1/2}$). To next order in ϵ,

$$\frac{\partial^2 X_2}{\partial \psi_0^2} + X_2 = \frac{\mathscr{D}}{\kappa^2}\left(\xi_0 X_1 + \frac{1}{\pi}\int_{-\infty}^{\infty} \frac{d\xi_0'}{\xi_0 + X_1 - \xi_0' - X_1'} + f \cos \psi_0\right) \tag{40}$$

The form of equation (40) for X_2 is that of a forced linear oscillator. In order for X_2 to be a periodic function of ψ_0, there must be no terms in a Fourier decomposition of the right-hand side (RHS) of equation (40) which contain $\cos \psi_0$ or $\sin \psi_0$ because such terms would resonantly give rise to a secular trend for X_2. This constraint requires

$$\oint (\text{RHS}) \cos \psi_0 \, d\psi_0 = 0 \quad \text{and} \quad \oint (\text{RHS}) \sin \psi_0 \, d\psi_0 = 0 , \tag{41}$$

yielding the following coupled nonlinear integral equations that determine the unknown functions $C(\xi_0) \equiv A(\xi_0) \cos \Phi(\xi_0)$ and $S(\xi_0) \equiv A(\xi_0) \sin \Phi(\xi_0)$:

$$\xi_0 C(\xi_0) + \frac{1}{\pi^2}\int_{-\infty}^{\infty} d\xi_0' \times \oint \frac{\cos \psi_0 \, d\psi_0}{(\xi_0 - \xi_0') + (C - C') \cos \psi_0 + (S - S') \sin \psi_0} - f = 0 , \tag{42a}$$

$$\xi_0 S(\xi_0) + \frac{1}{\pi^2}\int_{-\infty}^{\infty} d\xi_0' \times \oint \frac{\sin \psi_0 \, d\psi_0}{(\xi_0 - \xi_0') + (C - C') \cos \psi_0 + (S - S') \sin \psi_0} = 0 , \tag{42b}$$

where we have written C' for $C(\xi_0')$, etc.

The ψ_0 integrations in equations (42) may be performed analytically by first writing

$$(\xi_0 - \xi_0') + (C - C') \cos \psi_0 + (S - S') \sin \psi_0 \equiv (\xi_0 - \xi_0')[1 + q \cos (\psi_0 - \Delta)] , \tag{43}$$

where q and Δ are defined as functions of ξ_0 and ξ_0' through

$$q \cos \Delta \equiv \frac{C - C'}{\xi_0 - \xi_0'} \quad \text{and} \quad q \sin \Delta \equiv \frac{S - S'}{\xi_0 - \xi_0'} . \tag{44}$$

Now define $\vartheta \equiv \psi_0 - \Delta$, and recall the trigonometric identities

$$\cos \psi_0 = \cos \Delta \cos \vartheta - \sin \Delta \sin \vartheta , \tag{45a}$$

$$\sin \psi_0 = \sin \Delta \cos \vartheta + \cos \Delta \sin \vartheta . \tag{45b}$$

Switch the integration over a complete cycle in ψ_0 to one in ϑ from $-\pi$ to $+\pi$. Noting that the odd parts of the integrand give zero contributions, while (Gradshteyn and Ryzhik 1980, p. 366)

$$I_n(q) \equiv \frac{1}{2\pi}\int_{-\pi}^{\pi} \frac{\cos n\vartheta \, d\vartheta}{1 + q \cos \vartheta} = \frac{1}{q^n (1 - q^2)^{1/2}} [(1 - q^2)^{1/2} - 1]^n , \tag{46}$$

we obtain

$$\xi_0 C(\xi_0) + \frac{2}{\pi}\int_{-\infty}^{\infty} I_1(q) \cos \Delta \frac{d\xi_0'}{\xi_0 - \xi_0'} - f = 0 , \tag{47a}$$

$$\xi_0 S(\xi_0) + \frac{2}{\pi}\int_{-\infty}^{\infty} I_1(q) \sin \Delta \frac{d\xi_0'}{\xi_0 - \xi_0'} = 0 . \tag{47b}$$

The pair (47a) and (47b) may be written more compactly by multiplying equation (47b) by i and adding the result to equation (47a). After a little algebra, we get the fundamental integral equation of our problem,

$$\frac{1}{\pi}\int_{-\infty}^{\infty} I(q^2)\left[\frac{Z(\xi_0') - Z(\xi_0)}{(\xi_0' - \xi_0)^2}\right] d\xi_0' + \xi_0 Z(\xi_0) = f , \tag{48}$$

where we have defined the complex function Z of a real variable ξ_0 to be

$$Z(\xi_0) \equiv C(\xi_0) + iS(\xi_0) = A(\xi_0) e^{i\Phi(\xi_0)} , \tag{49}$$

where we have used equation (44) to write

$$qe^{i\Delta} = \frac{Z(\xi_0') - Z(\xi_0)}{\xi_0' - \xi_0} \tag{50}$$

and where we have defined

$$I(q^2) \equiv -\frac{2}{q} I_1(q) = \frac{2}{q^2}\left[(1-q^2)^{-1/2} - 1\right], \tag{51}$$

with q^2 given through equation (50) by

$$q^2 = \left|\frac{Z(\xi_0') - Z(\xi_0)}{\xi_0' - \xi_0}\right|^2. \tag{52}$$

In this form we see that q has an immediate geometrical interpretation, since it is the modulus of the relative radial displacement of two streamlines measured as a fraction of their original unperturbed spacing. Clearly, if q^2 were ever to become greater than or equal to unity, the corresponding streamlines would cross at some angular phase. This would happen first for neighboring streamlines, i.e., for the limit $\xi_0' \to \xi_0$; thus, the criterion for streamline crossing is whether the quantity

$$q_0 \equiv \left|\frac{dZ}{d\xi_0}\right| \tag{53}$$

ever reaches unity or larger. In § V we shall see that self-consistent (long) spiral density waves always adjust their properties so that $q_0 < 1$, i.e., so that *streamline crossing does not formally occur* (at least to the order of approximation considered here).

Equations (48), (51), and (52) constitute our basic set to solve for the complex Lagrangian displacement $Z(\xi_0)$. Once $Z(\xi_0)$ is known, we may obtain the physical displacement (in nondimensional form) as (cf. eqs. [39] and [49])

$$X(\xi_0, \psi_0) = \mathrm{Re}\left\{Z(\xi_0)e^{-i\psi_0}\right\}, \tag{54}$$

from which we may recover the surface density contrast (cf. eqs. [24], [30], and [34]):

$$\frac{\sigma}{\sigma_0} = \frac{1}{1 + \partial X/\partial\xi_0}. \tag{55}$$

The observed contrast is a function of $\varphi \approx \psi_0/m$ and the dimensionless *Eulerian* radial variable $\xi \equiv \epsilon^{-1/2}(r - r_L)/r_L$ given by

$$\xi = \xi_0 + X. \tag{56}$$

The plots in this paper are made for radial cuts, $\psi_0 = 0$ and $\psi_0 = \pi/2$, i.e., for $X = \mathrm{Re}\{Z(\xi_0)\}$ and $X = \mathrm{Im}\{Z(\xi_0)\}$.

c) *Recovery of Linear Theory*

The linear theory may be recovered from equation (48) by ignoring all effects of quadratic order or higher, i.e., by taking the limit $q^2 \to 0$. In this limit,

$$I(q^2) \to 1 \quad \text{as} \quad q^2 \to 0, \tag{57}$$

so that an integration by parts yields, for equation (48),

$$\frac{1}{\pi}\int_{-\infty}^{\infty} \frac{dZ/d\xi_0'}{\xi_0' - \xi_0}\, d\xi_0' + \xi_0 Z(\xi_0) = f. \tag{58}$$

The Cauchy integral in equation (58) can be performed by contour integration, yielding the ordinary differential equation

$$-i\frac{dZ}{d\xi_0} + \xi_0 Z(\xi_0) = f \tag{59}$$

that governs the propagation of linear trailing density waves from inner Lindblad resonance (cf. Shu 1984). The solution to equation (59), satisfying the boundary condition $Z = 0$ at $\xi = -\infty$ (far evanescent region), reads

$$Z_{\mathrm{linear}}(\xi_0) = (2\pi)^{1/2} f W(\xi_0), \tag{60a}$$

$$W(\xi_0) = i\frac{\exp(-i\xi_0^2/2)}{(2\pi)^{1/2}}\int_{-\infty}^{\xi_0} \exp\left(\frac{i\eta_0^2}{2}\right) d\eta_0. \tag{60b}$$

Figure 2 shows the real and imaginary parts of the normalized wave function $W(\xi_0)$ plotted against ξ_0. Notice that, as $\xi_0 \to +\infty$, $|W(\xi_0)| \to 1$, but the local wavenumber $|dW/d\xi_0| \to \xi_0$. Thus, even for $f \ll 1$, linear theory must break down for large enough ξ_0 because equation (53) implies that the (streamline-crossing) parameter

$$(q_0)_{\mathrm{linear}} = (2\pi)^{1/2} f \left|\frac{dW}{d\xi_0}\right| \tag{61}$$

will become of order unity at

$$\xi_0 \approx \frac{1}{(2\pi)^{1/2} f}. \tag{62}$$

III. WKBJ THEORY

a) *Nonlinear Dispersion Relation*

Another interpretation of equation (62) is that when f is $\sim(2\pi)^{-1/2}$, resonantly excited spiral density waves can become nonlinear within one inverse wavenumber of the position of exact resonance.[4] As we shall see explicitly in § IV, the nonlinear effects prevent the streamline crossings predicted by linear theory for large enough ξ_0. Many of the properties of the nonlinear waves in the far wave zone can, in fact, be extracted analytically by applying WKBJ techniques. For $\xi_0 \gg 1$, we expect the amplitude $A(\xi_0)$ to be much less quickly varying than the phase $\Phi(\xi_0)$ in equation (49). The wavy nature of Z accentuates the importance of local contributions (where $\xi_0' \approx \xi_0$) to the self-gravity integral of equation (48) because of the tendency of distant positive and negative contributions to cancel each other out. If we expand $\Phi(\xi_0')$ and $A(\xi_0')$ in a Taylor series about $\xi_0' = \xi_0$, we may write, to lowest WKBJ order,

$$Z(\xi_0') \approx Z(\xi_0)\exp\left[iK(\xi_0' - \xi_0)\right], \tag{63}$$

where K is the nondimensional wavenumber (for the Lagrangian displacement),

$$K \equiv \frac{d\Phi}{d\xi_0}, \tag{64}$$

and is *negative* in our sign convention for trailing waves.

To this WKBJ order, we may write

$$\frac{Z(\xi_0') - Z(\xi_0)}{\xi_0' - \xi_0} \approx Z(\xi_0)\left\{\frac{\exp\left[iK(\xi_0' - \xi_0)\right] - 1}{(\xi_0' - \xi_0)}\right\} = iKZ(\xi_0)e^{i\zeta}\frac{\sin\zeta}{\zeta}, \tag{65}$$

where

$$\zeta \equiv \tfrac{1}{2}K(\xi_0' - \xi_0). \tag{66}$$

[4] The relationship between our f and the parameter x_{NL} of Goldreich and Tremaine (1978) or Lissauer and Cuzzi (1982) is $x_{\mathrm{NL}} f = (\epsilon/2\pi)^{1/2}$.

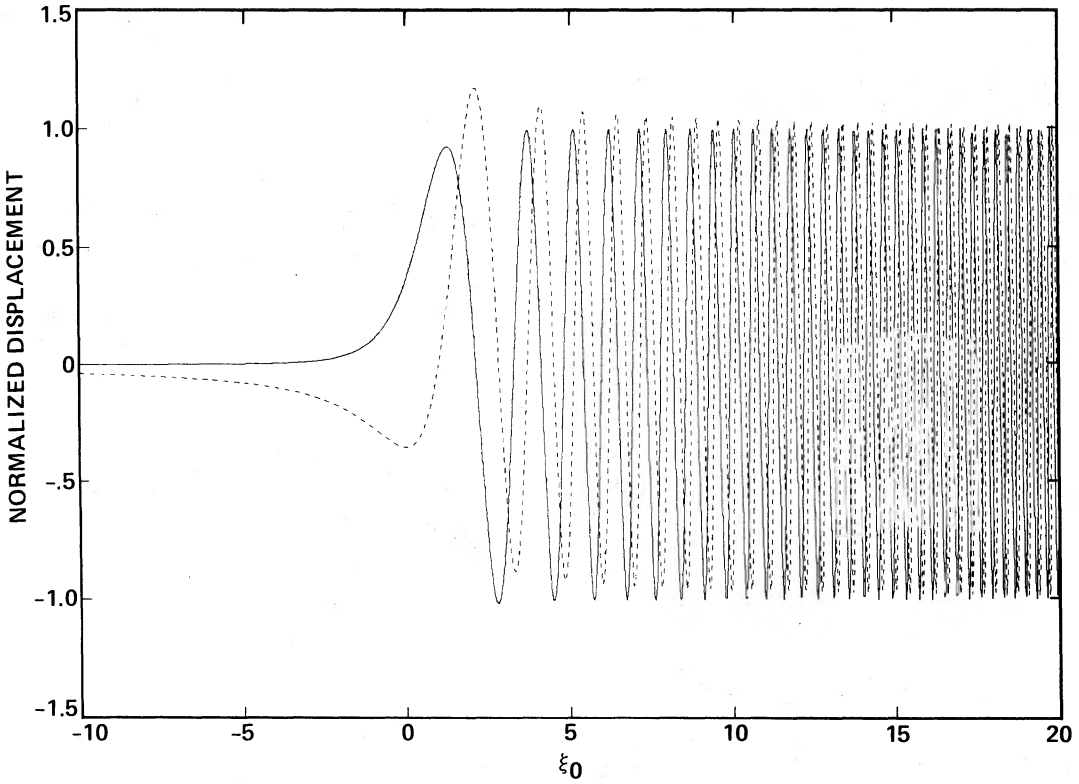

FIG. 2.—The real and imaginary parts of the linear wave function $W(\xi_0)$, defined by eq. (60b), where ξ_0 is the nondimensional distance from Lindblad resonance defined by eqs. (34) and (30).

Equations (52) and (53) may now be approximated as

$$q^2 \approx q_0^2 \frac{\sin^2 \zeta}{\zeta^2}, \tag{67a}$$

$$q_0^2 \approx K^2 A^2, \tag{67b}$$

and the self-gravity integral has the nonvanishing part

$$\frac{1}{\pi} \int_{-\infty}^{\infty} I(q^2) \left[\frac{Z(\xi_0') - Z(\xi_0)}{(\xi_0' - \xi_0)^2} \right] d\xi_0' \approx KZ(\xi_0) H(q_0^2), \tag{68a}$$

$$H(q_0^2) \equiv \frac{1}{\pi} \int_{-\infty}^{\infty} I(q^2) \frac{\sin^2 \zeta}{\zeta^2} d\zeta, \tag{68b}$$

where q^2 is given in terms of q_0 and ζ by equation (67a), and $I(q^2)$ is given by equation (51).

The substitution of equation (68a) into equation (48), when ξ_0 is taken to be very large (i.e., $\xi_0 Z \gg f$) results in the dispersion relation (we take K to be real and negative):

$$|K| H(q_0^2) = \xi_0, \tag{69}$$

which gives the (absolute value of the) wavenumber as a function of position ξ_0 when the amplitude A (or $q_0^2 = K^2 A^2$) is known. The properties of the integral function $H(q_0^2)$ are given in Appendix C; here we merely remark that it is a monotonically increasing function of its argument q_0^2, with the limiting values

$$H(q_0^2) \to 1 \quad \text{as} \quad q_0^2 \to 0, \tag{70a}$$

$$H(q_0^2) \to -\frac{2\sqrt{3}}{\pi} \ln (1 - q_0^2) \quad \text{as} \quad q_0^2 \to 1. \tag{70b}$$

b) Nonlinear Amplitude Relation

It is well known from linear density wave theory that the amplitude variation may be obtained either from a second-order WKBJ calculation or from a wave conservation principle (Toomre 1969; Shu 1970; Dewar 1972; Mark 1974; Goldreich and Tremaine 1979). We use the latter method here, i.e., we relate the amplitude A to the angular momentum transport.

Appendix A shows that the torque exerted by the moon in exciting the density waves is equal to

$$T = m \left(\frac{r_L^5 \mathscr{D}^2}{2G} \right) \epsilon^3 \mathscr{T}(\infty), \tag{71}$$

where $\mathscr{T}(\xi_0)$ for arbitrary ξ_0 is the nondimensional quantity

$$\mathscr{T}(\xi_0) \equiv -f \int_{-\infty}^{\xi_0} \text{Im} \{Z(\xi_0'')\} d\xi_0''. \tag{72}$$

(For inner Lindblad resonances, $\mathscr{T}$ is negative.) On the other hand, Appendix B shows that the nondimensional torque $\mathscr{T}(\xi_0)$ exerted up to the point ξ_0 must be carried away by an angular momentum luminosity (in density waves) through the disk whose nondimensional value is given by (S. Tremaine, 1983, private communication)

$$\mathscr{L}(\xi_0) = \int_{-\infty}^{\xi_0} d\xi_0'' \int_{\xi_0}^{\infty} d\xi_0' P(\xi_0'', \xi_0'), \tag{73}$$

where

$$P(\xi_0'', \xi_0') \equiv \frac{1}{2\pi i} \frac{I(q^2)}{(\xi_0' - \xi_0'')^2} [Z^*(\xi_0'') Z(\xi_0') - Z(\xi_0'') Z^*(\xi_0')] \tag{74}$$

and the asterisk denotes complex conjugation. In equation (74), q^2 is given by equation (52) except that ξ_0'' replaces ξ_0.

Equation (73) can be given the interpretation that the angular momentum luminosity across ξ_0 results from the interaction of the disk particles inside ξ_0 with those outside ξ_0. (In the linear context, Lynden-Bell and Kalnajs [1972] referred to this as the sum of lorry transport and gravitational torque.)

With ξ_0'' replacing ξ_0, equation (63) yields the approximation

$$\mathscr{L}(\xi_0) \approx -\frac{A^2(\xi_0)}{\pi}\int_{-\infty}^{\zeta_0} d\zeta'' \int_{\zeta_0-\zeta''}^{\infty} I(q^2)\frac{\sin 2\zeta}{\zeta^2}\,d\zeta\,, \qquad (75)$$

where $\zeta_0 \equiv -K\xi_0/2$, $\zeta'' \equiv -K\xi_0''/2$, and $\zeta \equiv -K(\xi_0' - \xi_0'')/2$, with $K < 0$ and q^2 given by equation (67a). Switching the order of integration in equation (75), we obtain

$$\mathscr{L}(\xi_0) = -\frac{A^2(\xi_0)}{\pi}\int_0^{\infty} d\zeta I(q^2)\frac{\sin 2\zeta}{\zeta^2}\int_{\zeta_0-\zeta}^{\zeta_0} d\zeta''\,. \qquad (76)$$

Performing the ζ'' integration, we get

$$\mathscr{L}(\xi_0) = -A^2(\xi_0)L(q_0^2)\,, \qquad (77a)$$

$$L(q_0^2) \equiv \frac{1}{\pi}\int_0^{\infty} I(q^2)\frac{\sin 2\zeta}{\zeta}\,d\zeta\,, \qquad (77b)$$

where q_0^2 is given by equation (67b). The properties of the integral function $L(q_0^2)$ are given in Appendix C. Here we merely note that it, like the integral $H_0(q_0^2)$, is also a monotonically increasing function of its argument q_0^2, but $L(q_0^2)$ has the limiting values

$$L(q_0^2) \to \tfrac{1}{2} \quad \text{as} \quad q_0^2 \to 0\,, \qquad (78a)$$

$$L(q_0^2) \to -\frac{2\sqrt{3}}{\pi}\ln(1-q_0^2) \quad \text{as} \quad q_0^2 \to 1\,, \qquad (78b)$$

i.e., $L(q_0^2) \to H(q_0^2)$ only for nearly crossing streamlines.

Equation (77a) may be regarded as an amplitude relation in the following sense. The torque (72) exerted by the moon on the disk is accumulated mostly within one wavelength of exact resonance (see § IV), so $\mathscr{T}$ tends (in an oscillatory manner) to a constant (negative) value as $\xi_0 \to \infty$. If someone were to give us this value (rather than require us to compute it by means of eq. [72]), the conservation principle, $\mathscr{L} = \mathscr{T}$, allows us to calculate the amplitude of the wave as a function of ξ_0 from

$$A^2(\xi_0)L(q_0^2) = -\mathscr{T}\,. \qquad (79)$$

To be more precise, if $\mathscr{T}$ is known, equations (67b), (69), and (79) give three relations to solve for the streamline-crossing parameter q_0, the wavenumber K, and the amplitude A, as functions of position ξ_0.

Since the torque $\mathscr{T}$ that can be exerted is finite, equation (79) requires A to be bounded. Equation (69) can then be satisfied as $\xi_0 \to +\infty$ only by requiring $|K| \to \infty$, or $q_0 \to 1$. In fact, both occur, so that when we divide equation (69) by equation (79), we obtain

$$\frac{|K|}{A^2} \to -\frac{\xi_0}{\mathscr{T}} \quad \text{as} \quad |K|A \to 1 \qquad (80)$$

because L and H are equal in the limit $q_0 \to 1$. In other words, in the far wave zone, nonlinear waves which are not viscously damped behave in the following way:

$$|K| \to \left(-\frac{\xi_0}{\mathscr{T}}\right)^{1/3} \quad \text{and} \quad A \to \left(-\frac{\mathscr{T}}{\xi_0}\right)^{1/3} \quad \text{as} \quad \xi_0 \to +\infty\,. \qquad (81)$$

This should be contrasted with the linear theory (obtained by assuming $q_0 \to 0$) where $|K| \to \xi_0$ and $A \to \text{constant} = (-2\mathscr{T})^{1/2} = (2\pi)^{1/2}f$ as $\xi_0 \to +\infty$.

In order to apply equations (81), we must know the value of the torque $\mathscr{T}$. This knowledge comes reliably only from solving the nonlinear wave excitation problem, especially in the partially evanescent and near wave zones (near $\xi_0 = 0$) that contribute the bulk of the integral on the right-hand side of equation (72). It is thus to the numerical solution of the wave equation (48) that we turn next.

IV. REPLACEMENT BY A DIFFERENTIAL EQUATION

a) *Motivation*

The singular and nonlinear nature of the integral equation (48) makes it rather nasty to tackle numerically. On either side of $\xi_0' = \xi_0$ are large contributions of opposite sign to the self-gravity integral. They cancel, leaving a small fraction of the original parts to be balanced by the rest of the equation. These difficulties are compounded in the far wave zone, where q^2 can be exceedingly close to 1 for neighboring streamlines, bringing on the singular behavior of the function $I(q^2)$ defined by equation (51). We are therefore strongly motivated to replace equation (48) by an alternative that would be easier to handle numerically.

Our hopes are buoyed by the reminder that, in the linear case, the integral equation can be rigorously reduced to an ordinary differential equation (see § IIc). Thus we are motivated to ask the following question. Can we write down an ordinary differential equation (of first order, preferably, in the complex function Z) which has the properties that (1) it reduces in the linear limit, $q_0 \to 0$ (which applies nearly everywhere for small f, and for the evanescent region $\xi_0 < 0$ for almost an f), to equation (59), and (2) it contains, in the asymptotic limit $\xi_0 \gg 1$, both the dispersion relation (69) and the amplitude relation (79)? The answer we discovered, by inspection, is yes. The desired equation—or more accurately, *a* usable equation—is

$$-2iL^{1/2}\frac{d}{d\xi_0}(L^{1/2}Z) + \frac{2L}{H}\xi_0 Z = f\,, \qquad (82)$$

where L and H are the integral functions of $q_0^2 = |dZ/d\xi_0|^2$ defined by equations (68b) and (77b) (see also Appendix C).

Clearly, equation (82) satisfies criterion 1 listed above, since $L \to \frac{1}{2}$ and $H \to 1$ in the limit $q_0 \to 0$. Moreover, if we multiply equation (82) by Z^* and take the imaginary part, we obtain

$$2\,\mathrm{Re}\left\{L^{1/2}Z^*\frac{d}{d\xi_0}(L^{1/2}Z)\right\} = f\,\mathrm{Im}\,(Z)\,. \qquad (83)$$

But the left-hand side of the above can be written as

$$L^{1/2}Z^*\frac{d}{d\xi_0}(L^{1/2}Z) + L^{1/2}Z\frac{d}{d\xi_0}(L^{1/2}Z^*) = \frac{d}{d\xi_0}(LZZ^*)\,, \qquad (84)$$

so that, with $ZZ^* = A^2$ and $Z = 0$ at $\xi_0 = -\infty$, the integration of equation (83) gives

$$L(q_0^2)A^2(\xi_0) = f\int_{-\infty}^{\xi_0} \mathrm{Im}\,\{Z(\xi_0')\}d\xi_0'\,,$$

which is equation (79). Finally, the substitution of $Z = Ae^{i\Phi}$ into equation (82), plus the assumption that A, H, and L are slowly varying in comparison with $e^{i\Phi}$, and the near-equality

$L \approx H$ for $\xi_0 \gg 1$, yield the approximation

$$-\frac{d\Phi}{d\xi_0} = \frac{\xi_0}{H(q_0^2)},$$

which is the dispersion relation (69) for $|K| = -d\Phi/d\xi_0 > 0$. This completes the verification that criteria 1 and 2 are satisfied.

We should emphasize that equation (82) has in no sense been *derived* from equation (48) under some rigorously statable set of assumptions. We have merely written it down as a heuristic equation which has many desirable properties; it is a *model* equation, not a physical one. However, the model is testable because its solution can be substituted back into equation (48) to see how well the latter is satisfied. We expect for moderate f that the satisfaction will be reasonable, since the model equation gives the correct description at both ends (ξ_0 large, negative or positive), so the middle ($|\xi_0| \sim 1$) is likely to work out too. If the "interpolation" fails, we may always regard the solution of the ordinary differential equation (82) as merely a means to generate a first iterate for the numerical solution of the integral equation (48).

Before we leave this subsection, we make one final comment. The differential equation (82) lends itself naturally to a simple Runge-Kutta scheme only if we define q_0 to be $A(-d\Phi/d\xi_0)$ rather than $|dZ/d\xi_0|$, where $Z \equiv Ae^{i\Phi}$. With this slight readjustment (which is justifiable since a *model* equation is always arbitrary to some extent), we can easily write down the system of first-order differential equations that govern Φ, A, and q_0. (In particular, one of the equations is simply $d\Phi/d\xi_0 = -q_0/A$.) We move now to a discussion of the numerical results.

b) Numerical Results

Figure 3 shows the solution of equation (82) for $f = 0.1$. Comparison with Figure 2 (cf. eq. [60a]) shows that nonlinear effects indeed do begin to manifest themselves after ξ_0 has attained values comparable to those given by equation (62). Figure 4 gives the associated nondimensional torque, $-\mathscr{T}$, as defined by equation (72). Notice that $-\mathscr{T}$ approaches, via damped oscillations, a constant asymptotic value which is very close to the value πf^2 implied by linear theory (see Appendix A). The total torque is accumulated mostly within one wavelength of exact resonance, where nonlinear effects are not very large and where compensating mechanisms (smaller amplitudes but longer wavelengths) are at work for the nonlinear effects which affect the torque. Figure 5, which plots the logarithm of the surface density contrast σ/σ_0 against the *Eulerian* variable $\xi = \xi_0 + X$, shows that nonlinear effects are most pronounced for observed optical depth profiles. In particular, because the peak-to-average densities are in the ratio $1/(1 - q_0)$, while the trough-to-average densities are in the ratio $1/(1 + q_0)$, we see that density waves can be strongly peaked when the streamline crossing parameter $q_0 \to 1$, as they are when $\xi_0 \to \infty$. By the same token, however, the trough densities can never drop below one-half the average value in the wave propagation region. We expect viscous effects to limit how closely q_0 can approach unity; thus, in a realistic calculation, the peaks are not likely to be nearly as strong as indicated by the inviscid theory presented here, although broad troughs, with $\sigma/\sigma_0 \gtrsim \frac{1}{2}$, will probably remain a feature of the more general theory.

Figure 6 indicates how well the solution to the differential

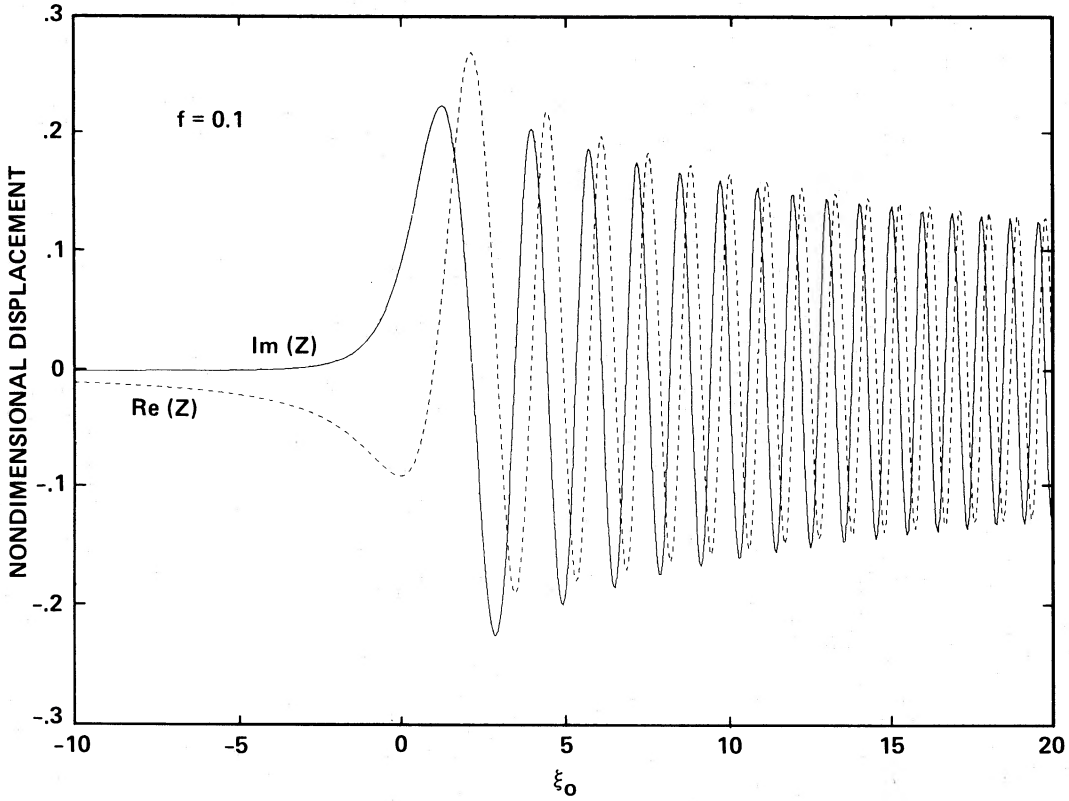

FIG. 3.—The real and imaginary parts of the Lagrangian displacement Z, for the case $f = 0.1$, as a function of the nondimensional (unperturbed) distance ξ_0 from resonance.

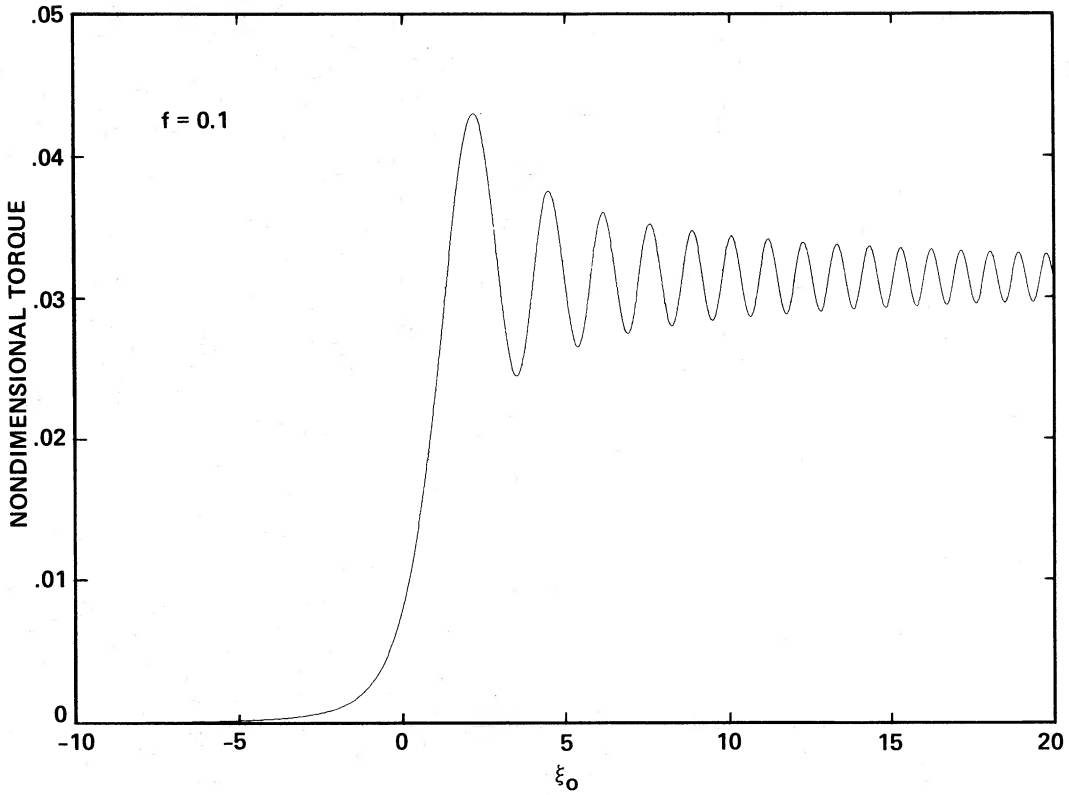

FIG. 4.—The accumulated nondimensional torque $-\mathscr{T}$, for the case $f = 0.1$, as a function of the nondimensional (unperturbed) distance ξ_0 from Lindblad resonance.

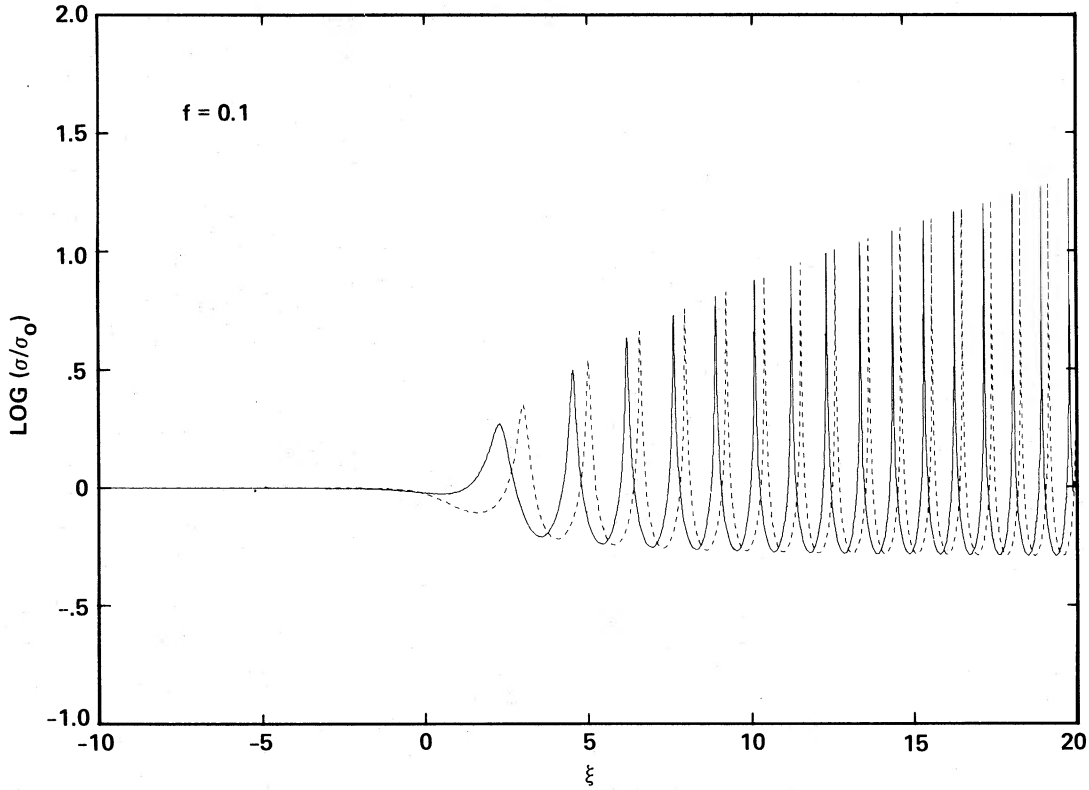

FIG. 5.—The normalized surface density σ/σ_0, for the case $f = 0.1$, of two radial cuts through the disk at orthogonal phases, as a function of the nondimensional Eulerian distance ξ from Lindblad resonance.

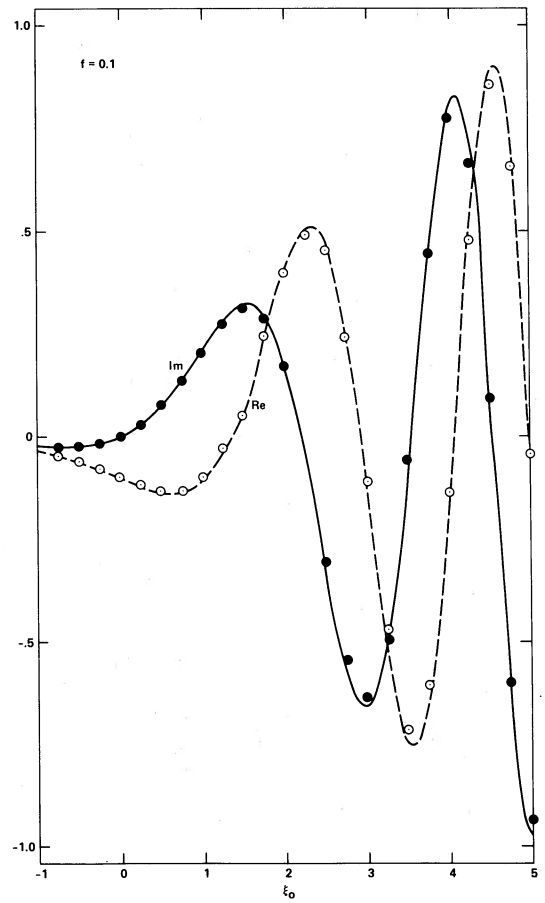

FIG. 6.—Measure of how well the solution of the differential equation (82) represents the solution of the integral equation (48) when $f = 0.1$. (See text for details.)

equation (82) satisfies the original integral equation (48):

$$\frac{1}{\pi}\int_{-\infty}^{\infty} I(q^2)\left[\frac{Z(\xi_0') - Z(\xi_0)}{(\xi_0' - \xi_0)^2}\right]d\xi_0' = -\xi_0 Z(\xi_0) + f. \quad (85)$$

The solid and dashed curves represent the imaginary and real parts of the right-hand side of equation (85) when the solution for $Z(\xi_0)$ from the differential equation (82) is substituted in it. The filled and open circles represent the imaginary and real parts of the left-hand side of equation (85) when the (principal-value) integral is evaluated at selected points ξ_0 by using the same solution for Z (see Appendix D for details). The good agreement between the filled circles and the solid curve and between the open circles and the dashed curve shows that the differential equation (82) gives a good representation of the integral equation (48) when $f = 0.1$ (or smaller).

Figures 7–10 display the same information as Figures 3–6, for $f = 0.5$. Notice from Figure 10 that the agreement between the circles and the curves is not as good; the fractional error reaches as high as 15% in the peaks and valleys. Nevertheless, the differential equation still gives a useful first approximation to the solution of the integral equation, and the main features of the wave profile in Figure 10 can be trusted. In particular, the increase in the wavelength because of nonlinear effects (compare Fig. 7 with Fig. 2), which prevents streamline crossing, is a general property of both the differential equation and the integral equation. Figure 8 shows that the accumulated torque $-\mathscr{T}$, even for this quite nonlinear case, has asymptotically almost its full linear value of πf^2. Table 2 gives the formal values for the torque ratio $T/T_{\rm lin}$ as a function of the forcing parameter f, but the precise values should not be given too much credence in light of the errors in the differential equation representation of the integral equation for $f = 0.5$ and larger. In particular, a direct attack on the integral equation is probably necessary to get reliable answers for $f \gtrsim 1$. Nevertheless, since most of the observed density waves in Saturn's rings are characterized by $f \lesssim 0.5$, one of the most important conclusions of this paper is that *nonlinear torques are not significantly smaller than their corresponding linear values, and therefore the difficulties with angular momentum transport time scales in the Saturn system cannot be relieved by appeal to nonlinear effects* (Goldreich and Tremaine 1982; Lissauer, Peale, and Cuzzi 1984; Borderies, Goldreich, and Tremaine 1984).

V. DISCUSSION

Because of the inviscid and pressure-free assumptions, we do not expect a good detailed correspondence between the theory developed so far and the nonlinear spiral density waves observed in nature; nevertheless, some preliminary comparisons are instructive. The peaky appearence of most of the observed density waves in Saturn's rings (e.g., Fig. 1) is a clear indication that the linear theory, which predicts sinusoidal variation, is inadequate (Lane *et al.* 1982; Holberg, Forrester, and Lissauer 1982; Esposito, O'Callaghan, and West 1983; Cuzzi *et al.* 1984). Peaked wavecrests had previously been encountered in the theory of spirally forced galactic shocks (Fugimoto 1968; Roberts 1969; Shu, Milione, and Roberts 1973), but, since streamlines never cross, shocks never formally occur for the resonantly forced, self-consistent, "long" waves studied in this paper (see also Vandervoort 1971). However, the very close packing of streamlines which occurs in the far wave zone yields "cusplike" solutions which are asymptotically close to the critical condition necessary to produce shocks. A similar situation seems to arise in Yuan's (1984) non-self-gravitating calculation of the response of interstellar gas in the "3 kpc arm" to an oval distortion in the central regions of the galaxy.

When streamlines come close but do not actually cross ($q_0 = 1-$), equations (53) and (55) predict that the troughs of the wave satisfy $\sigma/\sigma_0 \approx \frac{1}{2}$, explaining the broad, flat minima that appear in Figures 5 and 9. That the surface density in the troughs never falls below one-half the average ambient value seems consistent with observed optical depth profiles of nonlinear density waves in Saturn's rings (refer back to Fig. 1), but this point should be checked more carefully. Beyond this prediction, we cannot comment on any of the finer details of the observed wave profiles without modeling the effects of viscosity in limiting the asymptotic wave amplitudes to realistic values.

The most successful application of (linear) density wave

TABLE 2

NONLINEAR TORQUES

f	$-\mathscr{T}$	πf^2	$T/T_{\rm lin}$
0.1.....	0.03136	0.03142	0.9982
0.2.....	0.1251	0.1257	0.9957
0.5.....	0.7669	0.7854	0.9764
1.0.....	2.921	3.142	0.9297
2.0.....	10.63	12.57	0.8456
5.0.....	22.26	28.27	0.7873

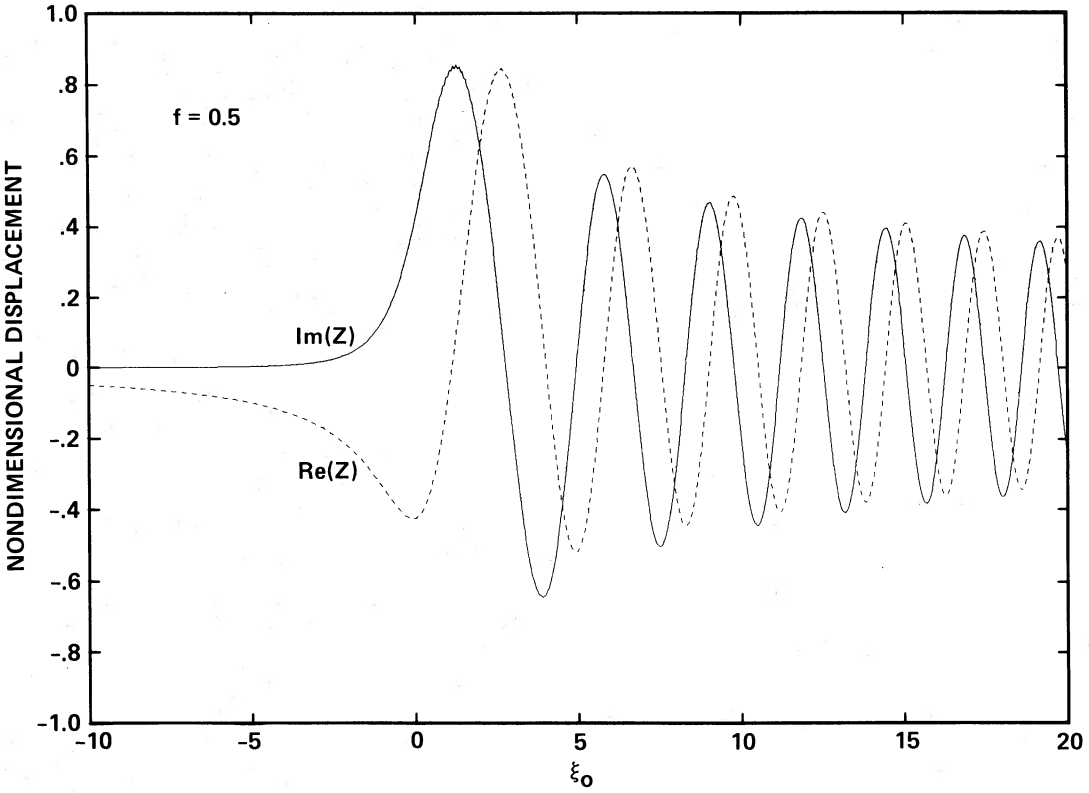

FIG. 7.—The real and imaginary parts of the Lagrangian displacement Z, for the case $f = 0.5$, as a function of the nondimensional (unperturbed) distance ξ_0 from resonance.

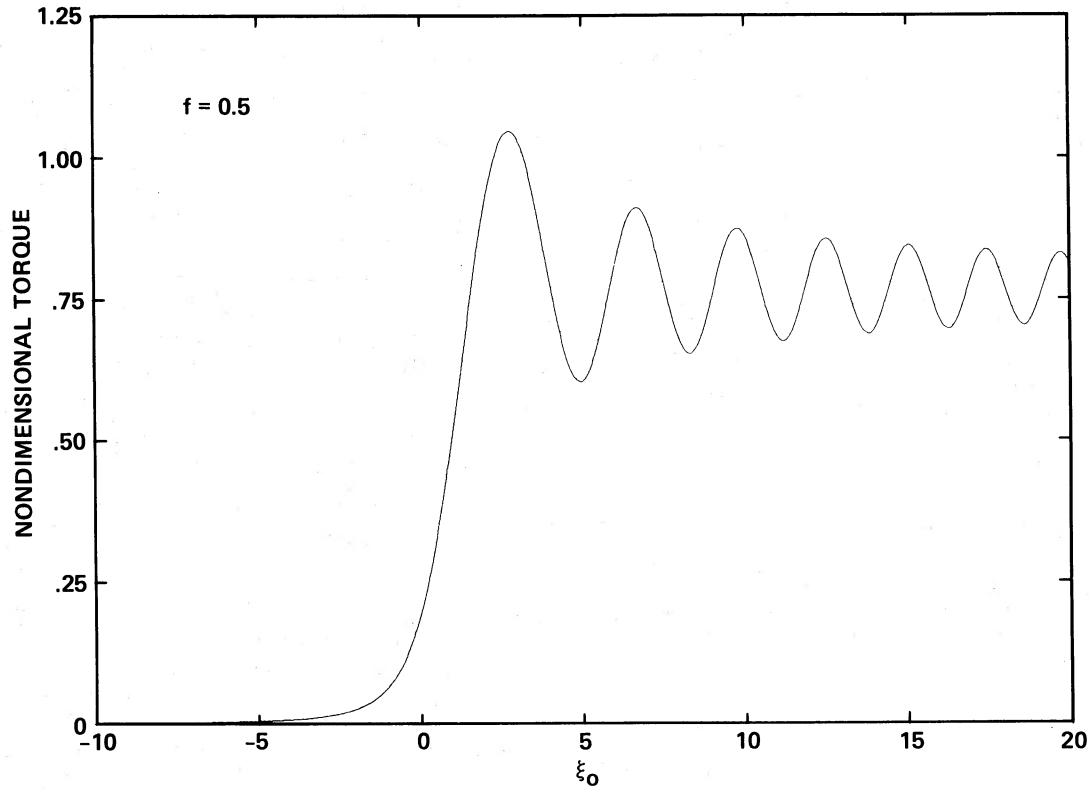

FIG. 8.—The accumulated nondimensional torque, $-\mathcal{T}$, for the case $f = 0.5$, as a function of the nondimensional (unperturbed) distance ξ_0 from Lindblad resonance.

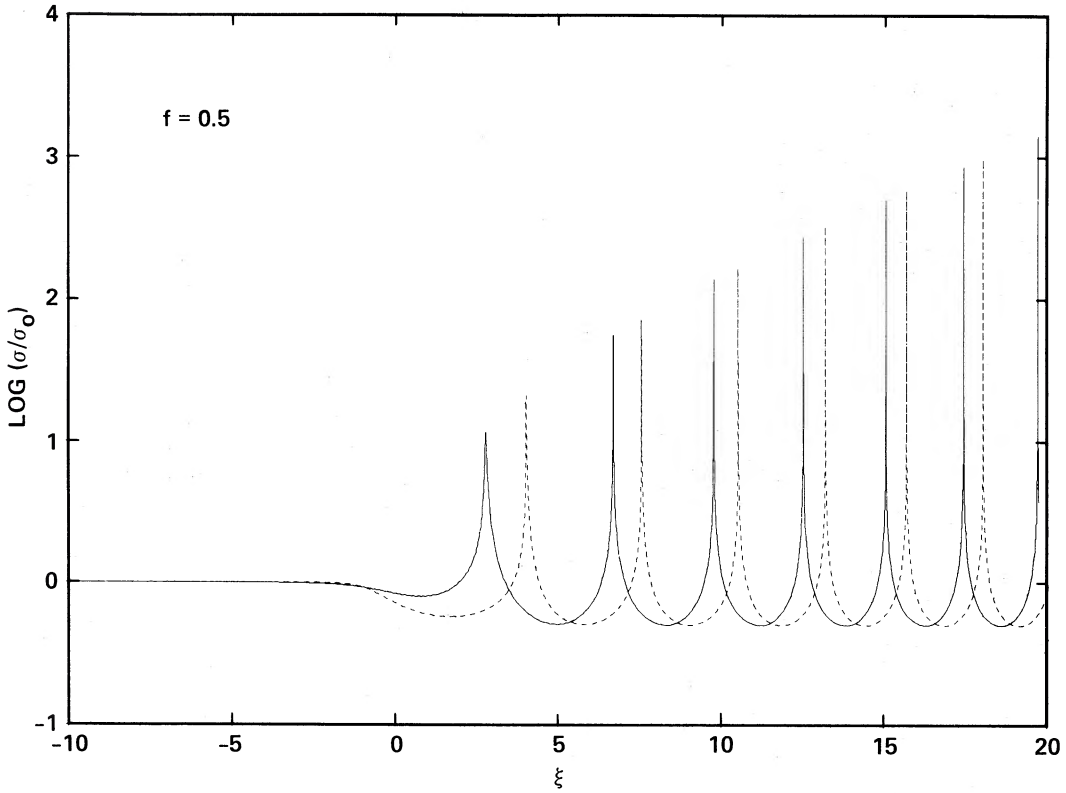

FIG. 9.—The normalized surface density σ/σ_0, for the case $f = 0.5$, of two radial cuts through the disk at orthogonal phases, as a function of the nondimensional Eulerian distance ξ from Lindblad resonance.

theory to Saturn's rings has been the derivation of local surface mass densities (e.g., Cuzzi, Lissauer, and Shu 1981; Lane *et al.* 1982), leading to fairly precise estimates of the overall ring mass (Holberg, Forrester, and Lissauer 1982; Holberg 1982; Cuzzi *et al.* 1984; Esposito *et al.* 1984). In the linear theory, the dispersion relationship predicts a local wavelength λ (spacing between successive crests) that is inversely proportional to the radial distance from resonance, with the coefficient yielding a measure of the surface density σ_0. Figure 11 shows that the relationship between wavelength and distance from resonance departs from the predictions of linear theory for a forcing amplitude of $f = 0.2$ typical of many of the observed waves in Saturn's rings. The departure is largest at large distances ξ, where the nonlinear inviscid theory (cf. eq. [81]) predicts $\lambda \propto \xi^{-1/3}$ instead of $\lambda \propto \xi^{-1}$. If inclusion of the effects of viscosity have the net effect of pinning down q_0 to some definite value smaller than unity (P. Goldreich 1983, private communication), then the relationship $\lambda \propto \xi^{-1}$ would be recovered, but the proportionality constant would be different from the relationship of linear density wave theory by a factor of $H(q_0^2)$ (see eq. [69]). Since $H(q_0^2) \geq 1$, it is possible that the surface mass densities in Saturn's rings have heretofore been systematically somewhat overestimated. Empirical determinations of the value of q_0 (from observed σ/σ_0 at the peaks) would allow one method of obtaining the correction factor $H(q_0^2)$ for this effect.

On the theoretical side, the biggest obstacle that remains to prevent detailed application to Saturn's rings is the proper incorporation of viscous effects. A powerful formalism for treating the effects of viscosity has been developed by Borderies, Goldreich, and Tremaine (1983*b*) in their attack on the problem of the resonant origin of sharp outer edges, and their technique should be equally useful in the present context. The incorporation of viscous effects would complete the program of using spiral density waves as a diagnostic of the physical state that prevails in Saturn's rings; however, it is becoming increasingly clear that the numerical value of viscosity derived for regions of wave propagation will probably not be representative of the disk as a whole, since the presence of the nonlinear wave itself (or of neighboring nonlinear waves, as is often the case in the A ring) tends to raise the viscosity above the value appropriate to an unperturbed disk. Nevertheless, the problem remains an intriguing theoretical challenge.

For application to spiral galaxies, the most important generalization would be the inclusion of the effects of finite velocity dispersion (which then introduces the possibility of "short" waves in addition to the "long" waves studied here). If this effect is simulated by the inclusion of a fluid pressure, with the gas remaining isothermal, we would need to add to the right-hand side of equation (14a) the term

$$\frac{c^2}{\sigma}\frac{\partial \sigma}{\partial r},$$

where c is the isothermal speed of sound. Appendix E then shows that this term ultimately results in an additional term on the left-hand side of equation (48) of the form

$$-\epsilon^{-1/2}\frac{\delta_1}{2}Q^2\frac{d}{d\xi_0}\left[I(q_0^2)\frac{dZ}{d\xi_0}\right], \tag{86}$$

where δ_1 and Q are defined by equations (1) and (2) and $I(q_0^2)$ is defined by equation (51) with q_0 replacing q. Since the pa-

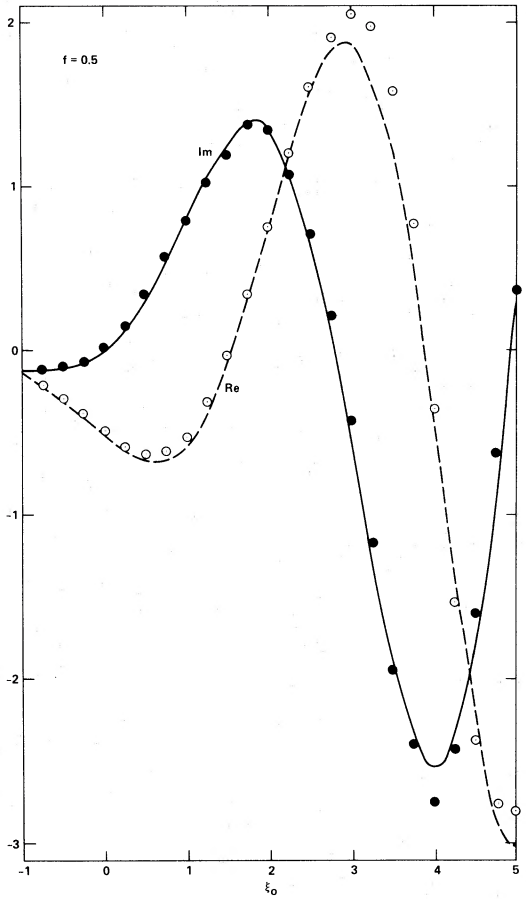

FIG. 10.—Measure of how well the solution of the differential equation (82) represents the solution of the integral equation (48) when $f = 0.5$. (See text for details.)

rameter δ_1 is of order ϵ (see eq. [33]), pressure effects are negligible in Saturn's rings unless $Q^2 I(q_0^2)$ is large (of order $\epsilon^{-1/2}$). This may happen in the far wave zone for some waves (where the viscosity is also important). For galaxies, ϵ is not such a small parameter, and the effects of finite velocity dispersion are always important. In this case the Taylor series expansion (31) is also of limited utility, and it is more informative to write the governing wave equation in the *dimensional* form

$$-c^2 \frac{d}{dr_0}\left[I(q_0^2)\frac{dR}{dr_0}\right] + 2G\sigma_0(r_0)\int_0^\infty I(q^2)\left[\frac{R(r_0') - R(r_0)}{(r_0' - r_0)^2}\right] dr_0' + [\kappa^2 - (\omega - m\Omega)^2]R = \frac{1}{r_0}\Psi_M(r_0)\,, \quad (87)$$

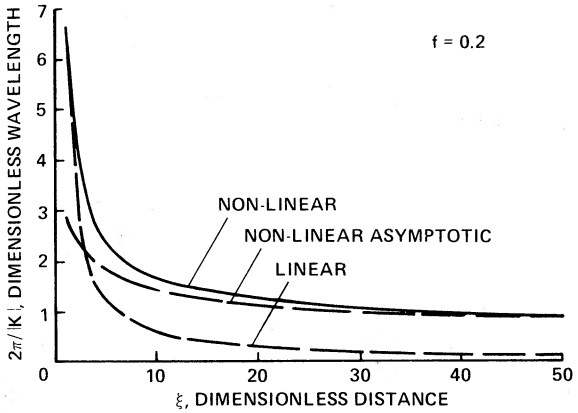

FIG. 11.—Relationship between the dimensionless wavelength, $2\pi|K|^{-1}$ (spacing between successive peaks), and the nondimensional distance ξ from Lindblad resonance for $f = 0.2$.

where $R(r_0)$ is the complex radial part of the Lagrangian displacement r_1 and

$$q^2 = \left|\frac{R(r_0') - R(r_0)}{r_0' - r_0}\right|^2,$$

with $q_0 = |dR/dr_0|$. Applied to a disk galaxy, Ψ_M could represent the forcing by a central bar or a (small) companion. Many (but not all) of the physical processes studied for spiral galaxies in the linear regime can be approached in the nonlinear context by means of equation (87). The inclusion of viscous terms would allow one to address related issues in protostellar nebulae and binary star accretion disks, as well as such problems as disk truncation and the like.

We are grateful to Scott Tremaine for his many helpful comments, in particular for his suggestion that total surface density be used instead of perturbational surface density in the calculation of the self-gravity, and for his derivation of the angular momentum transport that is the subject of Appendix B. Peter Goldreich contributed several penetrating insights, and discussions with Steve Balbus, Pat Cassen, Len Cowie, Jeff Cuzzi, Steve Lubow, and Sue Terebey were very useful to us, particularly in the formative stages of this project. We thank Larry Esposito for providing us with *Voyager* photopolarimeter observations of nonlinear density waves in Saturn's rings (Fig. 1) and Brian Hirano for programming assistance. This work was supported in part by NASA consortium grant NCA2-0R050-203 and by NSF grant AST 83-14682.

APPENDIX A

THE NONLINEAR TORQUE

In an Eulerian description, the torque T exerted by the moon on the entire disk can be calculated from

$$T = -\int_0^\infty r dr \oint d\theta \sigma(r, \theta, t)\frac{\partial V_M}{\partial \theta}(r, \theta, t)\,. \quad (A1)$$

The use of equation (22), with $\varphi = \theta - \Omega_p t$, allows us to convert the above to a Lagrangian calculation:

$$T = -\int_0^\infty r dr_0\, \sigma_0(r_0) \oint d\psi_0 \frac{\partial V_M}{\partial \varphi}, \tag{A2}$$

where $\partial V_M/\partial\varphi$ is to be evaluated at (r, φ), with r given by equation (9) and φ by equation (13). If we now write (cf. eq. [39])

$$r_1(r_0, \psi_0) = r_{1c}(r_0) \cos \psi_0 + r_{1s}(r_0) \sin \psi_0, \tag{A3a}$$

$$r_{1c} = \epsilon^{1/2} r_L \text{ Re } \{Z(\xi_0)\}, \qquad r_{1s} = \epsilon^{1/2} r_L \text{ Im } \{Z(\xi_0)\}, \tag{A3b}$$

we may integrate equation (26) to obtain

$$\varphi_1 = -\frac{m\phi_M \sin \psi_0}{r_0^2(\omega - m\Omega)^2} + \frac{2\Omega}{r_0(\omega - m\Omega)} (r_{1c} \sin \psi_0 - r_{1s} \cos \psi_0). \tag{A4}$$

Let $\psi_1 \equiv m\varphi_1$, and expand the smoothly varying function $\partial V_M/\partial\varphi$ with respect to the small quantities r_1 and ψ_1. To quadratic order in ϕ_M, r_1, or ψ_1, equation (A1) becomes

$$T = m\int_0^\infty \sigma_0(r_0) r_0\, dr_0 \oint d\psi_0 \left[\phi_M(r_0) + r_1 \frac{d\phi_M}{dr_0}\right](\sin \psi_0 + \psi_1 \cos \psi_0). \tag{A5}$$

The linear term $\phi_M \sin \psi_0$ integrates to zero over a complete cycle of ψ_0, as does the cubic term $r_1\psi_1(d\phi_M/dr_0) \cos \psi_0$, which is small in any case. With equations (A4) and (A5), we now have

$$T = m \int_0^\infty \sigma_0(r_0) r_0\, dr_0 \oint d\psi_0\, r_{1s}(r_0) \left[\frac{d\phi_M}{dr_0} \sin^2 \psi_0 - \frac{2m\Omega\phi_M}{r_0(\omega - m\Omega)} \cos^2 \psi_0\right], \tag{A6}$$

which upon integration over ψ_0 gives

$$T = m\pi \int_0^\infty \sigma_0(r_0) \left[r_0 \frac{d\phi_M}{dr_0} - \frac{2m\Omega\phi_M}{(\omega - m\Omega)}\right] r_{1s}(r_0) dr_0. \tag{A7}$$

We switch variables from r_0 to $\xi_0 \equiv \epsilon^{-1/2} (r_0 - r_L)/r_L$ and note that r_{1s} is a rapidly varying function of ξ_0 (cf. Fig. 2). Thus, we may approximate the rest of the integrand with its value at $r_0 = r_L$, and write equation (A7) as

$$T = -m\pi r_L^2 \sigma_0(r_L) \Psi_M(r_L) \epsilon \int_{-\infty}^\infty \text{Im } (Z) d\xi_0, \tag{A8}$$

where Ψ_M is defined by equation (20). The introduction of the symbols ϵ and f, as defined by equations (33) and (36), allows us to write equation (A8) in the form (71) quoted in the text.

To check formula (A8), we compute the linear torque (i.e., that which results from applying linear density wave theory). Consider the integral (whose imaginary part is of interest to us)

$$N \equiv \int_{-\infty}^\infty Z_{\text{linear}}\, d\xi_0, \tag{A9}$$

where Z_{linear} is given by equation (60a). Written out explicitly,

$$N = if \int_{-\infty}^\infty d\xi_0 \exp(-i\xi_0^2/2) \int_{-\infty}^{\xi_0} \exp(i\eta_0^2/2) d\eta_0. \tag{A10}$$

Take the complex conjugate of the above and switch the order of integration:

$$N^* = -if \int_{-\infty}^\infty d\eta_0 \exp(-i\eta_0^2/2) \int_{\eta_0}^\infty \exp(i\xi_0^2/2) d\xi_0. \tag{A11}$$

Interchange what we call ξ_0 and η_0 in equation (A11) and calculate

$$\text{Im } (N) \equiv \frac{1}{2i}(N - N^*) = \frac{f}{2} \int_{-\infty}^\infty \int_{-\infty}^\infty \exp[i(\eta_0^2 - \xi_0^2)/2] d\xi_0\, d\eta_0. \tag{A12}$$

If we rotate the axes by 45° by defining

$$y \equiv \frac{1}{\sqrt{2}}(\eta_0 - \xi_0), \quad x \equiv \frac{1}{\sqrt{2}}(\eta_0 + \xi_0), \tag{A13}$$

and note that the Jacobian of the transformation is

$$\frac{\partial(x, y)}{\partial(\xi_0, \eta_0)} = 1, \tag{A14}$$

we obtain

$$\text{Im}\,(N) = \frac{f}{2}\int_{-\infty}^{\infty}\int_{-\infty}^{\infty}\exp\,(ixy)dxdy\,. \tag{A15}$$

The integral over x gives $2\pi\delta(y)$; the integral over y then gives 2π. Therefore, Im $(N) = \pi f$. Since ϵ and f are defined by equations (33) and (36), equation (A8) can be written as

$$T_{\text{linear}} = -m\pi^2\,\frac{\sigma_0(r_L)}{\mathscr{D}}\,[\Psi_M(r_L)]^2\,, \tag{A16}$$

which is a result of Goldreich and Tremaine (1978, 1979). For the nonlinear problem, we will often express the actual torque (A8) as a fraction of the linear value (A16):

$$\frac{T}{T_{\text{linear}}} = \frac{1}{\pi f}\int_{-\infty}^{\infty}\text{Im}\,(Z)d\xi_0\,. \tag{A17}$$

One of the major results of § IV is that for $f \lesssim 1$ (which covers the forcing values encountered by all the *observed* density waves in Saturn's rings), the ratio (A17) is *not* very reduced from the value unity. Thus, although nonlinear effects are important for the observed wave profiles, they do not appreciably affect any of the torque considerations which have been made use of previously.

APPENDIX B

TRANSPORT OF ANGULAR MOMENTUM

In an inviscid self-gravitating disk, all of the torque resonantly deposited by an external moon must be carried away by the spiral density wave which is excited by the forced oscillations. The angular momentum luminosity may be calculated by a method due to Borderies, Goldreich, and Tremaine (S. Tremaine 1983, private communication). To motivate the derivation here, note that the nondimensional torque density (cf. eq. [72]) is equal to $-f$ times the imaginary part of Z. Since Im $(ZZ^*) = 0$ and Im $(Z^*) =$ $-$ Im (Z), if we multiply equation (48) by Z^* and take the imaginary part, we obtain

$$\frac{1}{\pi}\int_{-\infty}^{\infty}\frac{I(q^2)}{(\xi_0' - \xi_0)^2}\,\text{Im}\,\{Z^*(\xi_0)Z(\xi_0')\}d\xi_0' = -f\,\text{Im}\,\{Z(\xi_0)\}\,. \tag{B1}$$

Integrate the above from $-\infty$ to ξ_0, and introduce the symbol $\mathscr{T}$ for the partial dimensionless torque of equation (72). To avoid confusion, call the dummy integration variable ξ_0'' instead of ξ_0, and write Im $\{Z^*(\xi_0'')Z(\xi_0')\}$ as $[Z^*(\xi_0'')Z(\xi_0') - Z(\xi_0'')Z^*(\xi_0')]/2i$. Then

$$\int_{-\infty}^{\xi_0}d\xi_0''\int_{-\infty}^{\infty}P(\xi_0'',\,\xi_0')d\xi_0' = \mathscr{T}(\xi_0)\,, \tag{B2}$$

where $P(\xi_0'',\,\xi_0')$ is the function defined by equation (74), and q^2 is given by equation (52) except that ξ_0'' replaces ξ_0. To derive equation (73), notice that q^2 is even in parity with respect to the interchange of ξ_0' and ξ_0''; thus, $P(\xi_0'',\,\xi_0')$ is odd, i.e.,

$$P(\xi_0',\,\xi_0'') = -P(\xi_0'',\,\xi_0')\,. \tag{B3}$$

Consequently, if we interchange what we call ξ_0'' and ξ_0' in equation (B2) and use the property (B3), we obtain

$$-\int_{-\infty}^{\xi_0}d\xi_0'\int_{-\infty}^{\infty}P(\xi_0'',\,\xi_0')d\xi_0'' = \mathscr{T}(\xi_0)\,. \tag{B4}$$

The addition of equation (B2) to equation (B4) gives

$$2\mathscr{T}(\xi_0) = \int_{-\infty}^{\xi_0}\int_{-\infty}^{\infty}d\xi_0'\,P(\xi_0'',\,\xi_0') - \int_{-\infty}^{\xi_0}d\xi_0'\int_{-\infty}^{\infty}d\xi_0''\,P(\xi_0'',\,\xi_0')\,. \tag{B5}$$

The domains of integration of the first and second integrals are shown in Figure 12. The net contributions which do not cancel by symmetry considerations are therefore given by

$$2\mathscr{T}(\xi_0) = \int_{-\infty}^{\xi_0}d\xi_0''\int_{\xi_0}^{\infty}d\xi_0'\,P(\xi_0'',\,\xi_0') - \int_{-\infty}^{\xi_0}d\xi_0'\int_{\xi_0}^{\infty}d\xi_0''\,P(\xi_0'',\,\xi_0')\,. \tag{B6}$$

If we interchange what we call ξ_0' and ξ_0'' in the second integral and again use equation (B3), we obtain, upon division by 2,

$$\mathscr{T}(\xi_0) = \int_{-\infty}^{\xi_0}d\xi_0''\int_{\xi_0}^{\infty}d\xi_0'\,P(\xi_0'',\,\xi_0')\,. \tag{B7}$$

In accordance with the principle of conservation of angular momentum, the right-hand side of equation (B7) must represent the nondimensional angular momentum luminosity $\mathscr{L}(\xi_0)$ that is identified in equation (73).

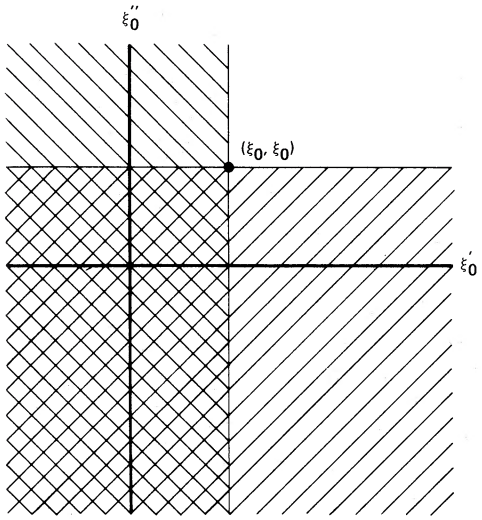

FIG. 12.—The domains of integration represented by the two integrals on the right-hand side of eq. (B5). In the crosshatched region of overlap, the contributions of the two integrals cancel.

APPENDIX C

THE FUNCTIONS $H(q_0^2)$ AND $L(q_0^2)$

To begin a discussion of the properties of the functions $H(q_0^2)$ and $L(q_0^2)$, defined respectively by equations (68b) and (77b), we first derive a relation between them. Write equation (68b) as

$$H(q_0^2) \equiv \frac{2}{\pi} \int_0^\infty I(q^2) \frac{\sin^2 \zeta}{\zeta^2} d\zeta , \tag{C1}$$

where $q = (q_0 \sin \zeta)/\zeta$, and integrate once by parts:

$$H(q_0^2) = \frac{2}{\pi} \int_0^\infty \frac{1}{\zeta} \frac{d}{d\zeta} [I(q^2) \sin^2 \zeta] d\zeta = 2L(q_0^2) + \frac{2}{\pi} \int_0^\infty \frac{\sin^2 \zeta}{\zeta} \frac{\partial I}{\partial \zeta} d\zeta , \tag{C2}$$

where

$$L(q_0^2) \equiv \frac{1}{\pi} \int_0^\infty I(q^2) \frac{\sin 2\zeta}{\zeta} d\zeta . \tag{C3}$$

Using the chain rule, we calculate

$$\frac{\partial I}{\partial \zeta} = \frac{dI}{dq} \frac{\partial q}{\partial \zeta} = \frac{\partial I}{\partial q_0} \frac{\zeta}{\sin \zeta} q_0 \left(\frac{\cos \zeta}{\zeta} - \frac{\sin \zeta}{\zeta^2} \right) = q_0 \frac{\partial I}{\partial q_0} \left(\frac{\cos \zeta}{\sin \zeta} - \frac{1}{\zeta} \right) ; \tag{C4}$$

thus equation (C2) becomes

$$H(q_0^2) = 2L(q_0^2) + q_0 \frac{dL}{dq_0} - q_0 \frac{dH}{dq_0} , \tag{C5}$$

which in turn can be written as

$$\frac{d}{dq_0} (q_0 H) = \frac{1}{q_0} \frac{d}{dq_0} (q_0^2 L) . \tag{C6}$$

If we multiply the above by q_0 and integrate from 0 to q_0, we obtain the desired relation,

$$L(q_0^2) = H(q_0^2) - \frac{1}{q_0^2} \int_0^{q_0} q_0' H(q_0'^2) dq_0' . \tag{C7}$$

This formula provides the most convenient way to evaluate $L(q_0^2)$ once we have tabulated $H(q_0^2)$.

The singularities, real and apparent, of $I(q^2)$, as defined by equation (51), make it inconvenient to calculate $H(q_0^2)$ directly from equation (C1). Instead, write equation (C1) out in full as

$$H(q_0^2) = \frac{2}{\pi}\int_0^\infty \frac{2}{q_0^2}\left[\left(1 - q_0^2\frac{\sin^2\zeta}{\zeta^2}\right)^{-1/2} - 1\right]d\zeta\,. \tag{C8}$$

Now note the identity

$$\left(1 - q_0^2\frac{\sin^2\zeta}{\zeta^2}\right)^{-1/2}d\zeta = d[\zeta^2 - q_0^2\sin^2\zeta)^{1/2}] + \frac{q_0^2}{2}\sin 2\zeta(\zeta^2 - q_0^2\sin^2\zeta)^{-1/2}d\zeta\,. \tag{C9}$$

The integration of the first term on the right-hand side of equation (C9) and the second term in the brackets of equation (C8) gives zero in the limits $\zeta = 0$ or $\zeta \to \infty$. Thus, equation (C8) becomes

$$H(q_0^2) = \frac{2}{\pi}\int_0^\infty \frac{\sin 2\zeta d\zeta}{(\zeta^2 - q_0^2\sin^2\zeta)^{1/2}}\,, \tag{C10}$$

which provides a convenient form for numerical computation.

For $q_0^2 < 1$, the function $H(q_0^2)$ may be expanded as the infinite series

$$H(q_0^2) = \sum_{n=0}^\infty \frac{(2n-1)!!}{n!2^n}A_n q_0^{2n}\,, \tag{C11}$$

where (Gradshteyn and Ryzhik 1980, p. 457)

$$A_n \equiv \frac{4}{\pi}\int_0^\infty \left(\frac{\sin\zeta}{\zeta}\right)^{2n+1}\cos\zeta d\zeta = 2(2n+1)\sum_{k=0}^n (-)^k\frac{(n+1-k)^{2n}}{k!(2n+1-k)!}\,. \tag{C12}$$

The corresponding series solution for $L(q_0^2)$ reads

$$L(q_0^2) = \sum_{n=0}^\infty \frac{(2n+1)!!}{(n+1)!2^{n+1}}A_n q_0^{2n}\,, \tag{C13}$$

as may easily be verified by substitution in equation (C6). The limiting values (70a) and (78a) follow directly from these expressions.

For q_0^2 near unity, the dominant contribution to the integral (C10) comes from $\zeta \approx 0$, where we may make the approximation $\sin 2\zeta \approx 2\zeta$ and expand:

$$\zeta^2 - q_0^2\sin^2\zeta = (1 - q_0^2)\zeta^2 + \frac{q_0^2}{3}\zeta^4 + \cdots \approx \beta^2\zeta^2 + \frac{\zeta^4}{3}\,,$$

with $\beta^2 \equiv 1 - q_0^2 \ll 1$. If we now divide the range of integration in equation (C10) into 0 to γ and γ to ∞, where $\beta \ll \gamma \ll 1$, we obtain

$$H(q_0^2) \approx \frac{4\sqrt{3}}{\pi}\,\mathrm{arcsinh}\left[\frac{\gamma}{(3\beta)^{1/2}}\right] + \frac{2}{\pi}\int_\gamma^\infty \frac{\sin^2\zeta d\zeta}{(\zeta^2 - \sin^2\zeta)^{1/2}}\,. \tag{C14}$$

The integral in equation (C14) is well behaved, while the first term on the right-hand side diverges logarithmically as $\beta \to 0$ in the manner prescribed by equation (70b). A similar set of manipulations applied to equation (C3) yields equation (78b).

When q_0^2 is neither very small nor very close to unity, it is more efficient to use contour integration (see Fig. 13) to turn the oscillatory integrand in (cf. eq. [C10])

$$H(q_0^2) = -\frac{i}{\pi}\int_{-\infty}^\infty \frac{e^{2i\zeta}d\zeta}{\zeta(1 - q_0^2\sin^2\zeta/\zeta^2)^{1/2}}$$

to a pole contribution minus a branch-cut contribution with an exponentially decaying integrand,

$$H(q_0^2) = \frac{1}{(1 - q_0^2)^{1/2}} - B(\eta_0)\,, \tag{C15}$$

where $\eta_0(q_0^2)$ is defined by the transcendental equation

$$q_0 = \frac{\eta_0}{\sinh\eta_0}\,, \tag{C16}$$

and the branch-cut contribution is

$$B(\eta_0) \equiv \frac{2}{\pi}\sinh\eta_0\int_{\eta_0}^\infty \frac{e^{-2\eta}d\eta}{(\eta_0\sinh^2\eta - \eta^2\sinh^2\eta_0)^{1/2}}\,. \tag{C17}$$

Notice that $B(\eta_0)$ vanishes in the linear limit $q_0 \to 0$ because the branch point $\zeta = i\eta_0$ then moves infinitely far off the real axis.

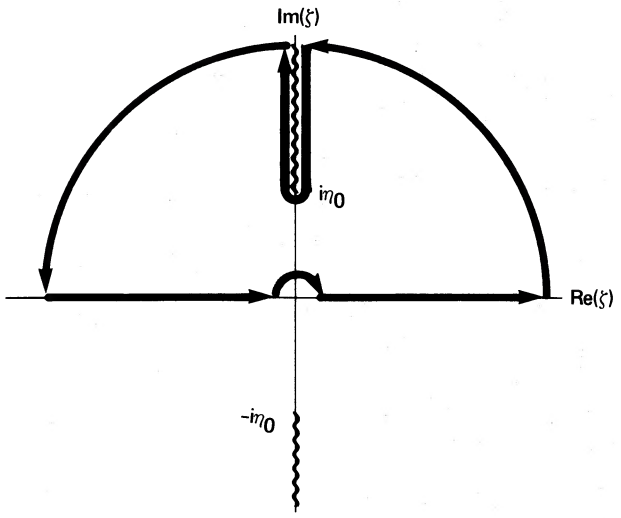

FIG. 13.—The contour in the complex ζ-plane that is needed to turn eq. (C10) into eq. (C15). There is a simple pole at $\zeta = 0$, and branch points at $\zeta = \pm i\eta_0$, where η_0 is defined through eq. (C16).

Using the formulae derived above, we have tabulated the functions $H(q_0^2)$ and $L(q_0^2)$ for a variety of values of q_0^2 between 0 and 1. To an accuracy better than a fraction of a percent, the values so tabulated can be fitted throughout this range by the analytical fitting formulae

$$H(q_0^2) = -\frac{4\sqrt{3}}{\pi} \ln \beta + \beta - aq_0^2 + bq_0^4 - cq_0^6 , \tag{C18a}$$

$$L(q_0^2) = H(q_0^2) - \frac{1}{q_0^2}\left[\frac{\sqrt{3}}{\pi}(q_0^2 + 2\beta^2 \ln \beta) + \frac{1}{3}(1 - \beta^3)\right] + \frac{a}{4} q_0^2 - \frac{b}{6} q_0^4 + \frac{c}{8} q_0^6 , \tag{C18b}$$

where $\beta = (1 - q_0^2)^{1/2}$ and $a = 0.12041$, $b = 0.005659$, $c = 0.17194$. The formulae (C18) allow the rapid step-by-step integration of equation (82).

APPENDIX D

CHECKING THE INTEGRAL EQUATION

Once a solution $Z(\xi_0)$ of the ordinary differential equation (82) has been generated, it behooves us to check how well it satisfies the original integral equation (48). This numerical check is complicated, however, by the large cancellations that occur in the neighborhood of $\xi_0' = \xi_0$ (see the discussion of § IV*b*). Clearly, it would be desirable to divide the range of integration on the left-hand side of equation (85) into $-\infty$ to $\xi_0 - \delta$, $\xi_0 - \delta$ to $\xi_0 + \delta$, and $\xi_0 + \delta$ to $+\infty$, where δ is some small but finite number (say, 0.01), and to evaluate the central piece

$$\frac{1}{\pi}\int_{\xi_0-\delta}^{\xi_0+\delta} I(q^2)\left[\frac{Z(\xi_0') - Z(\xi_0)}{(\xi_0' - \xi_0)^2}\right] d\xi_0' \tag{D1}$$

by a more careful technique than the standard integration schemes. The technique we used is the following. For given ξ_0, define a new integration variable $u \equiv \xi_0' - \xi_0$. From the stored data points (on a grid) for $Z(\xi_0')$, calculate the function

$$F(u) \equiv I(q^2)\left[\frac{Z(\xi_0') - Z(\xi_0)}{\xi_0' - \xi_0}\right], \tag{D2}$$

where q^2 is given by equation (52). Construct the odd part of this function,

$$F_{\rm odd}(u) = \tfrac{1}{2}[F(u) - F(-u)] , \tag{D3}$$

and fit the tabulated data by the polynomial

$$F_{\rm odd}(u) = F_1 u + F_3 u^3 + F_5 u^5 . \tag{D4}$$

In terms of $F_{\rm odd}(u)$, the principal-value integral (D1) can be expressed as

$$\frac{2}{\pi}\int_0^{\delta} [F_{\rm odd}(u)] du = \frac{2}{\pi}\left(F_1 \delta + F_3 \frac{\delta^3}{3} + F_5 \frac{\delta^5}{5}\right), \tag{D5}$$

a formula which is well matched by a four-step Runge-Kutta scheme to integrate the ordinary differential equation (82) and a fourth-order quadrature method to evaluate the rest of the left-hand side of equation (85).

APPENDIX E

INCLUSION OF PRESSURE

Given the approximate Lagrangian equation of continuity,

$$\sigma dr \approx \sigma_0 dr_0 , \tag{E1}$$

or the equivalent relation (24), we may express an isothermal pressure term as

$$-\frac{c^2}{\sigma}\frac{\partial\sigma}{\partial r} \approx -\frac{c^2}{\sigma_0}\frac{\partial\sigma}{\partial r_0} \approx -c^2\frac{\partial}{\partial r_0}\left(\frac{1}{1+\partial r_1/\partial r_0}\right), \tag{E2}$$

if we assume that $\sigma_0(r_0)$ is slowly varying. In the nondimensional variables introduced in § II*b*, this becomes

$$-\frac{c^2}{\sigma}\frac{\partial\sigma}{\partial r} = -\epsilon^{-1/2}\frac{c^2}{r_L}\frac{\partial}{\partial\xi_0}\left(\frac{1}{1+\partial X/\partial\xi_0}\right). \tag{E3}$$

In accordance with equations (37) and (39), the term to be differentiated with respect to ξ_0 in equation (E3) is, to lowest order in ϵ,

$$\left(1+\frac{dC}{d\xi_0}\cos\psi_0+\frac{dS}{d\xi_0}\sin\psi_0\right)^{-1}, \tag{E4}$$

which, subjected to the operation (41), gives the two additional terms

$$\frac{1}{\pi}\oint\frac{\cos\psi_0\, d\psi_0}{1+q_0\cos(\psi_0-\Delta_0)} = 2I_1(q_0)\cos\Delta_0 , \tag{E5a}$$

$$\frac{1}{\pi}\oint\frac{\sin\psi_0\, d\psi_0}{1+q_0\cos(\psi_0-\Delta_0)} = 2I_1(q_0)\sin\Delta_0 , \tag{E5b}$$

where $I_1(q_0)$ is defined through equation (46) and where

$$q_0\cos\Delta_0 = \frac{dC}{d\xi_0}, \qquad q_0\sin\Delta_0 = \frac{dS}{d\xi_0}. \tag{E6}$$

When the right-hand side of equation (E5b) is multiplied by i and added to the right-hand side of equation (E5a), we obtain

$$2I_1(q_0)e^{i\Delta_0} = \frac{2}{q_0}I_1(q_0)\frac{dZ}{d\xi_0} = -I(q_0^2)\frac{dZ}{d\xi_0}, \tag{E7}$$

where $I(q_0^2)$ is defined through equation (51), except that q_0 replaces q. The differentiation of the term (E7) and multiplication by the appropriate coefficients in accordance with equation (E3) lead to the addition of the term (86) to the left-hand side of equation (48). The derivation of equation (87) then follows in a straightforward manner.

REFERENCES

Bertin, G. 1980, *Phys. Repts.*, **61**, 1.
Borderies, N., Goldreich, P., and Tremaine, S. 1982, *Nature*, **299**, 209.
———. 1983*a*, *A.J.*, **88**, 226.
———. 1983*b*, *Icarus*, **55**, 124.
———. 1984, in *Planetary Rings*, ed. R. Greenberg and A. Brahic (Tucson: University of Arizona Press), p. 713.
Cuzzi, J. N., Lissauer, J. J., Esposito, L. W., Holberg, J. B., Marouf, E. A., Tyler, G. L., and Boischot, A. 1984, in *Planetary Rings*, ed. R. Greenberg and A. Brahic (Tucson: University of Arizona Press), p. 73.
Cuzzi, J. N., Lissauer, J. J., and Shu, F. H. 1981, *Nature*, **292**, 703.
Dewar, R. L. 1972, *Ap. J.*, **174**, 301.
Esposito, L. W., Cuzzi, J. N., Holberg, J. B., Marouf, E. A., Tyler, G. L., and Porco, C. C. 1984, in *Saturn*, ed. T. Gehrels and M. S. Mathews (Tucson: University of Arizona Press), p. 463.
Esposito, L. W., O'Callaghan, M., and West, R. A. 1983, *Icarus*, **56**, 439.
Fugimoto, M. 1968, in *IAU Symposium 29, Nonstable Phenomena in Galaxies*, ed. V. Ambartsumian (Yerevan: Academy of Sciences, Armenian SSR), p. 453.
Goldreich, P., and Tremaine, S. 1978, *Icarus*, **34**, 240.
———. 1979, *Ap. J.*, **233**, 857.
———. 1982, *Ann. Rev. Astr. Ap.*, **20**, 249.
Gradshteyn, I. S., and Ryzhik, I. M. 1980, *Tables of Integrals, Series, and Products* (New York: Academic).
Hohl, F. 1971, *Ap. J.*, **168**, 343.
Holberg, J. B. 1982, *A.J.*, **87**, 1416.
Holberg, J. B., Forrester, W. J., and Lissauer, J. J. 1982, *Nature*, **293**, 115.
Lane, A. L., *et al.* 1982, *Science*, **215**, 537.
Lin, C. C., and Bertin, G. 1984, in *IAU Symposium 106, The Milky Way*, ed. H. van Woerden, W. B. Burton, and R. J. Allen (Dordrecht: Reidel), in press.
Lin, C. C., and Lau, Y. Y. 1979, *Studies Appl. Math.*, **60**, 97.
Lin, C. C., and Shu, F. H. 1964, *Ap. J.*, **140**, 646.
Lindblad, B. 1963, *Stockholm Obs. Ann.*, **21**, No. 8.
Lissauer, J. J., Peale, S. J., and Cuzzi, J. N. 1984, *Icarus*, **58**, 159.
Lynden-Bell, D., and Kalnajs, A. J. 1972, *M.N.R.A.S.*, **157**, 1.
Mark, J. W.-K. 1974, *Ap. J.*, **193**, 539.
Miller, R. H., Prendergast, K. H., and Quirk, W. J. 1970, *Ap. J.*, **161**, 903.
Norman, C. A. 1978, *M.N.R.A.S.*, **182**, 457.
Roberts, W. W. 1969, *Ap. J.*, **158**, 123.
Sanders, R. H., and Huntley, J. M. 1976, *Ap. J.*, **209**, 53.
Sellwood, J., and Carlberg, R. 1984, *Ap. J.*, **282**, 61.
Shu, F. H. 1970, *Ap. J.*, **160**, 99.
———. 1984, in *Planetary Rings*, ed. R. Greenberg and A. Brahic (Tucson: University of Arizona Press), p. 513.
Shu, F. H., Milione, V., and Roberts, W. W. 1973, *Ap. J.*, **183**, 819.
Toomre, A. 1964, *Ap. J.*, **139**, 1217.
Toomre, A. 1969, *Ap. J.*, **158**, 899.

Toomre, A. 1981, in *The Structure and Evolution of Normal Galaxies*, ed. M. Fall and D. Lynden-Bell (London: Cambridge University Press), p. 111.
Toomre, A., and Toomre, J. 1972, *Ap. J.*, **178**, 623.
Vandervoort, P. O. 1971, *Ap. J.*, **166**, 37.
Woodward, P. R. 1980, private communication.
Yuan, C. 1984, *Ap. J.*, **281**, 600.

FRANK H. SHU: Astronomy Department, University of California, Berkeley, CA 94720

JACK J. LISSAUER and CHI YUAN: Mail Stop 245-3, NASA/Ames Research Center, Moffett Field, CA 94035